nature communications

Article

https://doi.org/10.1038/s41467-024-51542-z

FOXO-regulated OSER1 reduces oxidative stress and extends lifespan in multiple species

Received: 22 October 2022

Accepted: 12 August 2024

Published online: 21 August 2024

Check for updates

Jiangbo Song[1,10], Zhiquan Li[2,10], Lei Zhou[1], Xin Chen[1], Wei Qi Guinevere Sew[3], Héctor Herranz[3], Zilu Ye[4,5], Jesper Velgaard Olsen[4], Yuan Li[2], Marianne Nygaard[6,7], Kaare Christensen[6,7,8], Xiaoling Tong[1], Vilhelm A. Bohr[2,9], Lene Juel Rasmussen[2] ✉ & Fangyin Dai[1] ✉

FOXO transcription factors modulate aging-related pathways and influence longevity in multiple species, but the transcriptional targets that mediate these effects remain largely unknown. Here, we identify an evolutionarily conserved FOXO target gene, Oxidative stress-responsive serine-rich protein 1 (*OSER1*), whose overexpression extends lifespan in silkworms, nematodes, and flies, while its depletion correspondingly shortens lifespan. In flies, overexpression of OSER1 increases resistance to oxidative stress, starvation, and heat shock, while OSER1-depleted flies are more vulnerable to these stressors. In silkworms, hydrogen peroxide both induces and is scavenged by OSER1 in vitro and in vivo. Knockdown of OSER1 in *Caenorhabditis elegans* leads to increased ROS production and shorter lifespan, mitochondrial fragmentation, decreased ATP production, and altered transcription of mitochondrial genes. Human proteomic analysis suggests that OSER1 plays roles in oxidative stress response, cellular senescence, and reproduction, which is consistent with the data and suggests that OSER1 could play a role in fertility in silkworms and nematodes. Human studies demonstrate that polymorphic variants in *OSER1* are associated with human longevity. In summary, OSER1 is an evolutionarily conserved FOXO-regulated protein that improves resistance to oxidative stress, maintains mitochondrial functional integrity, and increases lifespan in multiple species. Additional studies will clarify the role of OSER1 as a critical effector of healthy aging.

Recent investigations into the molecular basis of aging suggest that the FOXO transcription factor family is a critical regulator of genes that modulate aging, lifespan, and the response to oxidative stress[1,2]. FOXO proteins modulate signaling pathways downstream of insulin/insulin-like growth factor-1 (IGF-1)[3], AMPK[4], TOR[5,6], JNK, and dietary restriction (DR)[7], and integrate signals from these pathways[8]. FOXO-regulated genes and pathways are widely implicated in age-related diseases such as cancer[9], Alzheimer's disease[10,11], and type 2 diabetes mellitus[12].

Elevated oxidative stress is associated with cancer[13], chronic kidney disease[14], and neurodegeneration[15]. FOXO proteins regulate and are regulated by redox level and oxidative stress[16]. For example, FOXOs upregulate catalase (CAT)[17], manganese superoxide dismutase (MnSOD)[18], and sestrins[19–21] while suppressing the expression of

A full list of affiliations appears at the end of the paper. ✉e-mail: lenera@sund.ku.dk; fydai@swu.edu.cn

https://doi.org/10.1038/s41467-024-51542-z

mitochondrial genes[22] and regulating the oxidative DNA damage response[23].

A multitude of FOXO target genes have been identified and characterized in *Caenorhabditis elegans* (*C. elegans*)[24], *Drosophila melanogaster* (*D. melanogaster*)[25], mouse[26], and human cells[27], or by meta-analysis and comparative multi-species "-omics"[28]. Nevertheless, many FOXO-regulated genes and their biological roles remain poorly characterized. Meanwhile, an emerging experimental system such as silkworm (*Bombyx mori, B. mori*) could potentially reveal the identity of conserved pro-longevity genes that cannot be readily identified in the more commonly used experimental model systems such as yeast, worms, flies, and mice. In this work, we identify and characterize a

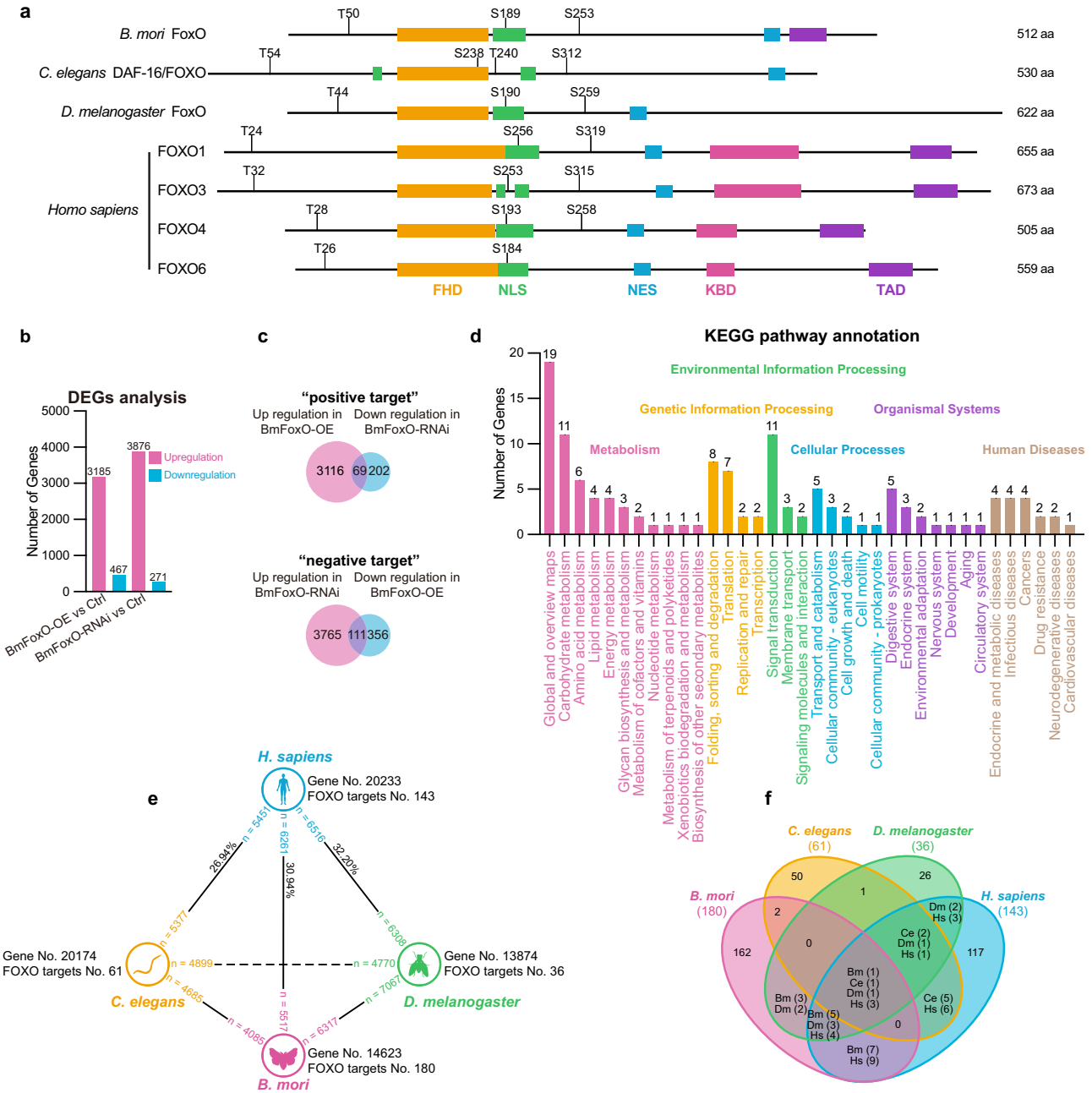

Fig. 1 | Identification of transcriptional targets of BmFoxO. a The secondary structure of FoxO proteins among *B. mori*, *C. elegans*, *D. melanogaster*, and *Homo sapiens*. Members in the FoxO family share a highly conserved forkhead DNA-binding domain (FHD), one or two nuclear localization signal(s) (NLS), a nuclear export signal (NES), and a transactivation domain (TAD). The KIX-binding domain (KBD) is only found in human FOXOs in this comparison. The presence of the FHD, KBD, and TAD was predicted using the NCBI Conserved Domains Database (NCBI CDD). The identification of NLS and NES was carried out with NLStradamus and LocNES, respectively. *C. elegans* and *D. melanogaster* FoxO do not have a functional TAD. The positions of Akt phosphorylation sites indicated were analyzed using NetPhos 3.1 Server. **b** BmN-SWU1 cells were selected for stable overexpression of *BmFoxO*^{CA} (constitutively active) or siRNA targeting *BmFoxO*. Total RNA was isolated for transcriptomic analysis, and differentially-expressed genes (DEGs) were identified. **c** Genes with up-regulated mRNA levels in BmFoxO overexpression and down-regulated in the BmFoxO knockdown conditions were denoted as "positive targets"; the opposite pattern was designated as "negative targets". **d** KEGG analyses of DEGs showing the DEGs involvement in metabolism, genetic/environmental information processing, human diseases, organismal systems, and cellular processes. **e** Bioinformatic analysis of orthologous genes among silkworm, nematode, *Drosophila*, and humans. **f** Venn diagram of FOXO transcriptional direct targets in the indicated species. All data are available in Supplementary Data 1, 2, and 3.

https://doi.org/10.1038/s41467-024-51542-z

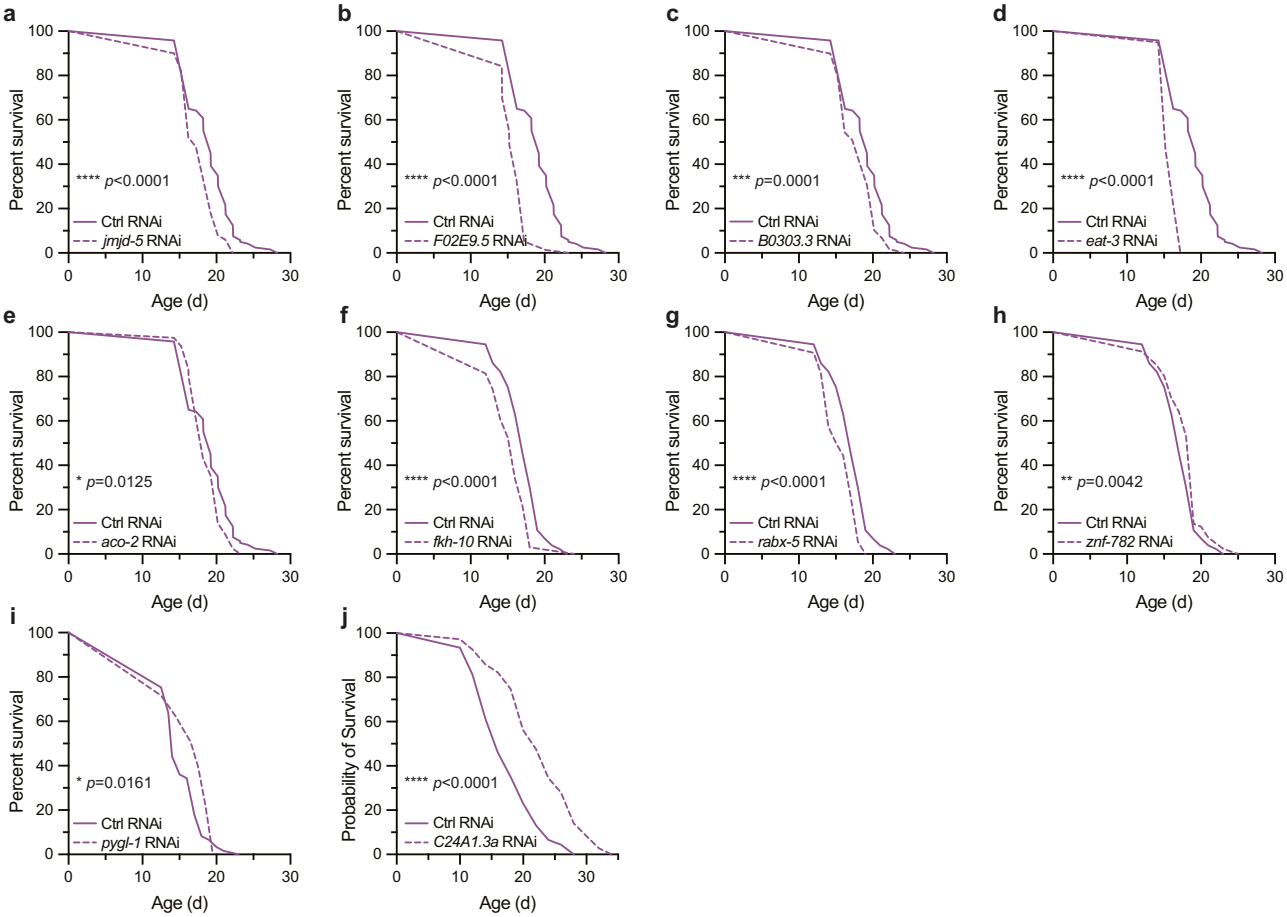

Fig. 2 | The survival analysis of 10 siRNA-mediated gene knockdowns in *C. elegans*. **a**–**g** *C. elegans* knockdowns that show shortened lifespan (*jmjd-5*, $n = 50$; *F02E9.5*, $n = 76$; *B0303.3*, $n = 59$; *eat-3*, $n = 119$; *aco-2*, $n = 79$; *fkh-10*, $n = 97$; *rabx-5*, $n = 54$). **h**–**j** *C. elegans* knockdowns that show extended lifespan (*znf-782*, $n = 81$; *pygl-1*, $n = 53$; *C24A1.3a*, $n = 107$). Controls for **i**, $n = 61$, for **j**, $n = 107$. The knockdowns of **a**-**e** were performed simultaneously to compare better the lifespan changes, so the same control ($n = 120$) was used and presented in the figure. Panels **f**–**h** also share the same controls ($n = 130$). Survival curves were plotted and analyzed by Log-rank (Mantel-Cox) test using GraphPad Prism 9. $^{*}p < 0.05$, $^{**}p < 0.01$, $^{***}p < 0.001$, $^{****}p < 0.0001$. Lifespan experiments were performed at least three times independently with similar observations. Source data are provided as a Source Data file.

FOXO target, Oxidative stress-responsive serine-rich protein 1 (OSER1), whose up- or downregulation increases or decreases lifespan, respectively, in *B. mori*, *C. elegans*, and *D. melanogaster*. A potential influence of OSER1 on human lifespan is supported by human subject studies.

Results

Transcriptomic analysis of FOXO targets

Comparative analysis of FOXOs between *B. mori*[29] and *C. elegans*, *D. melanogaster*, and *Homo sapiens* revealed highly conserved structural features like a forkhead DNA-binding domain (FHD), nuclear localization signals (NLS), and a transactivation domain (TAD)[16] (Fig. 1a) as well as their tertiary structures (Supplementary Fig. 1a, b), which confers the possibility of employing silkworm for FOXO targets screening. To screen FOXO transcriptional targets in silkworms, plasmids harboring wild-type *BmFoxO* or siRNA targeting *BmFoxO* were constructed (Supplementary Fig. 2) and transfected into silkworm BmN-SWU1 cells, in which BmFoxO was up- or down-regulated, respectively, as expected (Supplementary Fig. 3a–d). However, wild-type BmFoxO was predominantly overexpressed in BmN-SWU1 cells as an inactive cytosolic phosphorylated form (Supplementary Fig. 3e). To solve this problem, a constitutively active BmFoxO mutant ($BmFoxO^{CA}$) was transfected into and overexpressed in BmN-SWU1 cells. The $BmFoxO^{CA}$ mutant lacks AKT phosphorylation sites and is primarily expressed in the nucleus of BmN-SWU1 cells (Supplementary Fig. 3a, b, d, f). Subsequently, we identified 3185 upregulated and 467 downregulated transcripts in cells overexpressing $BmFoxO^{CA}$, while 3876 transcripts were upregulated and 271 were downregulated in BmFoxO-depleted cells (Fig. 1b and Supplementary Data 1) out of the whole transcriptome covering 14,623 genes[30]. We identified 69 genes that were upregulated by overexpression of BmFoxO and downregulated by knockdown of BmFoxO (i.e., positive targets), and 111 genes that were downregulated by overexpression of BmFoxO and upregulated in knockdown cells (i.e., negative targets) (Fig. 1c; Supplementary Fig. 4). Gene Ontology (GO) analysis revealed that these genes are involved in diverse cellular functions (Supplementary Fig. 5a), and KEGG analysis suggested roles in metabolism, genetic and environmental information processing, and multiple organismal and cellular processes (Fig. 1d). Several genes were linked to human diseases (Fig. 1d; Supplementary Data 2). Further investigation indicated roles in the TCA cycle, protein processing, and the PI3K-Akt signaling pathway (Supplementary Fig. 5b). Bioinformatic analyses showed that 30.94% of human genes have orthologous genes in silkworms, while nematode and *Drosophila* genes have known human orthologs (accounts for 26.94% and 32.20% of human genome, respectively) (Fig. 1e). Interestingly, of the 180 BmFoxO core targets identified in the transcriptomic analysis shown in Fig. 1c, 18 targets are conserved and 162 targets were either silkworm-specific or not yet reported in other species (Fig. 1f and Supplementary Data 3).

https://doi.org/10.1038/s41467-024-51542-z

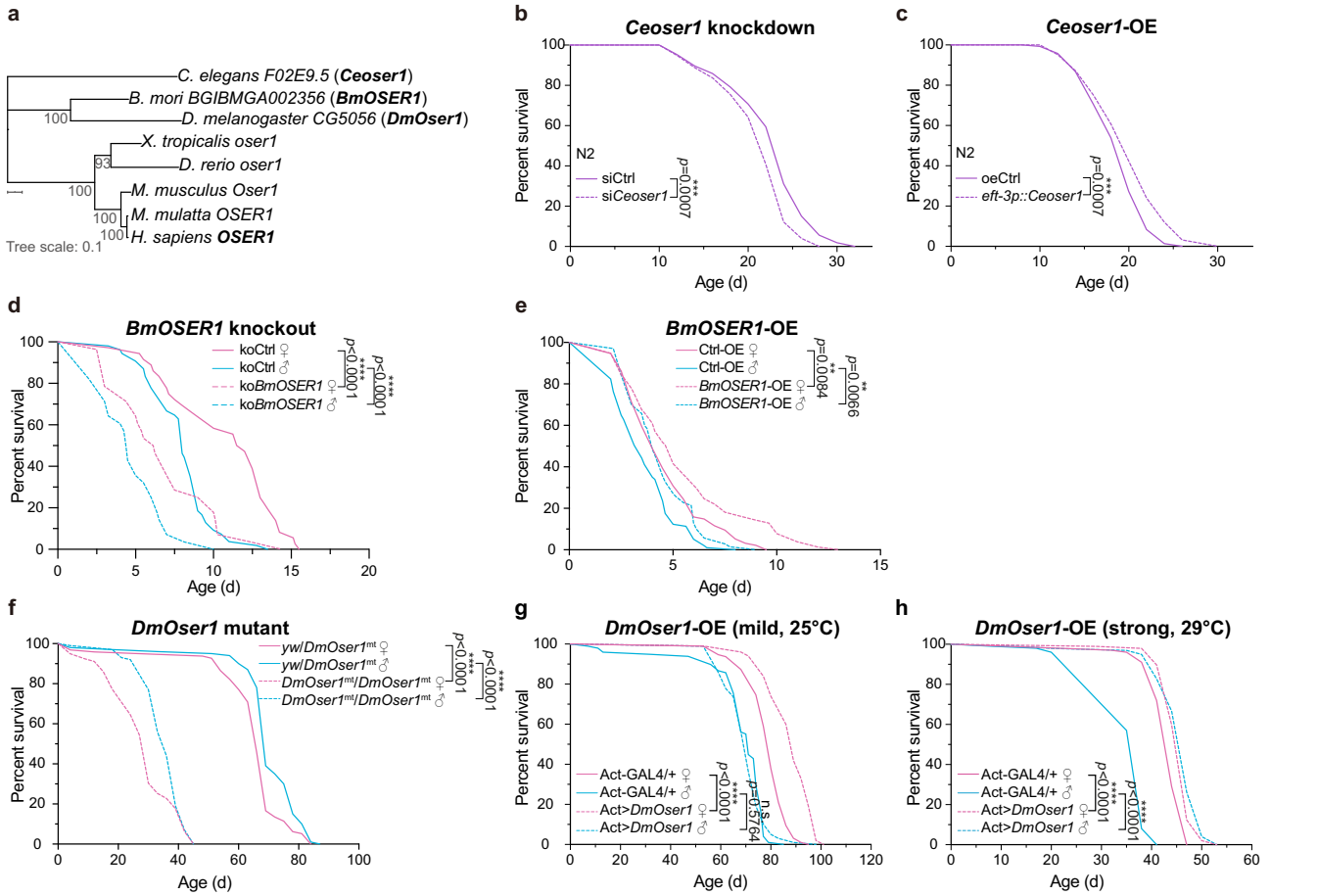

Fig. 3 | The effect of *OSER1* overexpression or knockdown on lifespan in nematodes, silkworms, and fruit flies. a Phylogeny of *OSER1* in *C. elegans*, *B. mori*, *D. melanogaster*, *Xenopus tropicalis*, *Danio rerio*, *Mus musculus*, *Macaca mulatta*, and *Homo sapiens*. The phylogenetic tree was generated with MEGA version 11.0.11. The scale bar 0.1 represents the number of substitutions per site. The lifespan of nematodes with *Ceoser1* knockdown (**b**: siCtrl, $n = 109$; siCeoser1, $n = 101$) or overexpression (**c**: oeCtrl, $n = 143$; siCeoser1, $n = 101$). The lifespan of *B. mori* with *BmOSER1* knockout (**d**: koCtrl ♀, $n = 36$; koCtrl ♂, $n = 54$; koBmOSER1 ♀, $n = 28$) or overexpression (**e**: Ctrl-OE ♀, $n = 94$; Ctrl-OE ♂, $n = 97$; BmOSER1-OE ♀, $n = 77$; BmOSER1-OE ♂, $n = 70$). The lifespan of heterozygotes control (yw/DmOser1) and *DmOser1* mutant flies (**f**: yw/DmOser1 ♀, $n = 96$; yw/DmOser1mt ♂, $n = 100$; DmOser1mt/DmOser1mt ♀, $n = 79$; DmOser1mt/DmOser1mt ♂, $n = 100$) or flies with mild (25 °C, **g**) (Act-GAL4/+ ♀, $n = 95$; Act-GAL4/+ ♂, $n = 98$; Act>DmOser1 ♀, $n = 100$; Act>DmOser1 ♂, $n = 99$) or strong overexpression of *DmOser1* (29 °C, **h**) (Act-GAL4/+ ♀, $n = 100$; Act-GAL4/+ ♂, $n = 100$; Act>DmOser1 ♀, $n = 97$; Act>DmOser1 ♂, $n = 99$). Survival curves were plotted and analyzed by Log-rank (Mantel-Cox) test using GraphPad Prism 9. n.s not significant. $^{**}p < 0.01$, $^{***}p < 0.001$, $^{****}p < 0.0001$. Lifespan experiments were performed at least three times independently with similar observations. Source data are provided as a Source Data file.

OSER1 extends lifespan in multiple species

To confirm the direct regulation of putative gene targets by BmFoxO, a 3 kb genomic DNA sequence in the upstream promoter region of candidate BmFoxO target genes was searched for the consensus FOXO binding motif, revealing possible matches in 42 of 180 putative target genes (Supplementary Table 1). Twenty-four of these genes have orthologs in *C. elegans* that were not reported as *daf-16* targets previously (Supplementary Data 4), and nine out of the other 18 genes have orthologs in humans and mice (Supplementary Table 2). To investigate the biological functions of these putative FOXO-regulated genes, single-gene siRNA knockdown was performed in *C. elegans*, and the lifespan of the knockdown and control strains was measured. The results show that knockdown of 7 genes shortened lifespan (*jmjd-5*, *F02E9.5*, *B0303.3*, *eat-3*, *aco-2*, *fkh-10*, *rabx-5*) while knockdown of 3 genes (*znf-782*, *pygl-1*, *C24A1.3a*) increased lifespan (Fig. 2; Supplementary Fig. 6; Supplementary Data 4). Knockdown of *F02E9.5* (*C. elegans* ortholog of silkworm *BGIBMGA002356* gene) had the largest impact of all putative FOXO targets, causing lifespan to decrease by 17% (Fig. 2b and Supplementary Data 4). Having identified the positively-regulated target of BmFoxO, *BGIBMGA002356* and its *C. elegans* ortholog, as a candidate for a conserved longevity gene, we searched for orthologous genes in other species. Phylogenetic analysis revealed that this gene is conserved from *C. elegans* to humans with the homologous genes forming four clusters (*i.e.*, nematode, insect, amphibian and fish, mammals), all of which share one protein domain of unknown function (DUF776) (Fig. 3a). As the human homolog was previously identified as Oxidatively-induced Serine-rich Protein 1 (OSER1), we adopted the following naming convention: *B. mori BGIBMGA002356, BmOSER1*; *C. elegans F02E9.5*, *Ceoser1*; *D. melanogaster CG5056*, *DmOser1* (Fig. 3a).

Additional analyses showed that depletion or overexpression of *Ceoser1* in wildtype N2 nematodes decreases or increases lifespan, respectively (Fig. 3b, c). Similarly, knockout of *BmOSER1* by CRISPR-Cas9 (Supplementary Fig. 7) shortened silkworm lifespan (Fig. 3d), which is consistent with the effect of *BmOSER1* knockdown (Supplementary Fig. 8a–d), while overexpression of *BmOSER1* increased lifespan (Fig. 3e and Supplementary Fig. 8e). Moreover, under conditions that promote low or high expression of *DmOser1*, the average lifespan of flies was correspondingly shorter or longer, respectively (Fig. 3f–h and Supplementary Fig. 9). We noted that overall lifespan is extended

https://doi.org/10.1038/s41467-024-51542-z

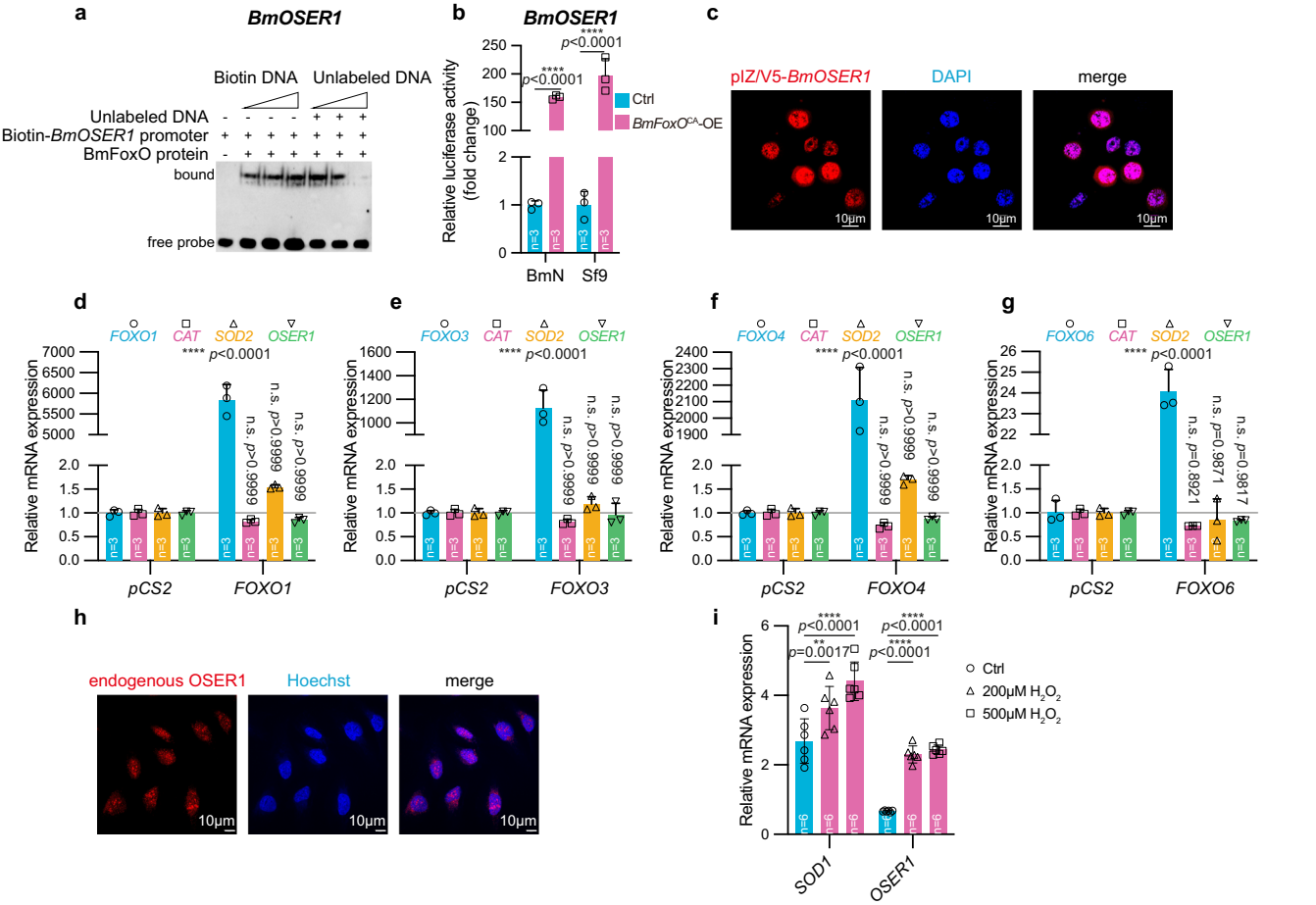

Fig. 4 | Regulation of OSER1 by FOXO in silkworms and humans. a EMSA using biotin-labeled *BmOSER1* promoter fragment and BmFoxO protein, as described in supplementary methods. **b** Dual-luciferase reporter gene assay quantifies transactivation of the luciferase reporter gene with co-expression of $BmFoxO^{CA}$, as described in methods. Data are presented as mean with SD and statistically tested by Two-way ANOVA. **c** Immunofluorescence analysis of BmOSER1 subcellular localization in BmN-SWU1 cells. Red, pIZ/V5-BmOSER1-DsRed2. Blue, DAPI for nucleus stain. Magenta, the merge of BmOSER1 and DAPI. Objective lens magnification, 100X. Scale bar, 10 μm. **d**–**g** The mRNA expression levels of Catalase (*CAT*), *SOD2*, and *OSER1* were detected by RT-qPCR with transfection of human *FOXO1* (**d**), *FOXO3* (**e**), *FOXO4* (**f**), and *FOXO6* (**g**) overexpression plasmids in U2OS cells. The relative mRNA expression was normalized to empty vector (pCS2) transfection control. Data are presented as mean with SD of three biological replicates and statistically tested by Two-way ANOVA. **h** Immunofluorescence staining showed that endogenous OSER1 localizes in the cell nucleus of U2OS cells. Red: OSER1, Blue, Hoechst. Scale bar, 10 μm. The images were taken by confocal laser scanning microscope LSM710 (Zesis) under 63X objective. **i** Relative *SOD1* and *OSER1* mRNA expression in U2OS cells treated with 0, 200, or 500 μM hydrogen peroxide (H_2O_2) for 12 h, respectively. Data are presented as mean with SD and statistically tested by Two-way ANOVA. n.s., not significant; $^{**}p < 0.01$, $^{***}p < 0.001$, $^{****}p < 0.0001$. All data points derive from independent cell line lysates. Source data are provided as a Source Data file.

when *DmOser1* is mildly overexpressed in females, but the maximal lifespan were extended in both male and female flies (Fig. 3g and Supplementary Fig. 9d–f). In contrast, lifespan was extended in both sexes when *DmOser1* was highly overexpressed (Fig. 3h and Supplementary Fig. 9g–i). These data demonstrate that OSER1 is a conserved regulator of longevity in nematodes, silkworms, and flies.

OSER1 is a target of FOXO

As mentioned above, the sequence 3 kb upstream of the *BmOSER1* start codon includes potential BmFoxO binding sites (Supplementary Table 1). To explore whether BmFoxO protein binds to these sequences in vitro, electrophoretic mobility shift assays (EMSA) were performed using purified BmFoxO protein and a biotin-labeled *BmOSER1* DNA fragment in the absence or presence of excess unlabeled competitor DNA (Fig. 4a). The results demonstrate specific binding of BmFoxO protein to the promoter of *BmOSER1*. To evaluate the functional consequences of this interaction, the putative *BmOSER1* promoter region (from 1 kb upstream of the *BmOSER1* ORF to the start codon) was cloned into the upstream of the luciferase reporter gene in vector pGL3 and used in a dual-luciferase reporter assay (Supplementary Fig. 2) without or with co-expression of $BmFoxO^{CA}$. The results show that expression of *BmOSER1* is dramatically induced in *B. mori* cells that overexpress $BmFoxO^{CA}$ (Fig. 4b). Furthermore, similar results were observed when the same experiment was performed in *Spodoptera frugiperda* Sf9 cells (Fig. 4b). Confocal microscopy showed that BmOSER1 primarily localizes to the cell nucleus (Fig. 4c), which was also observed in human U2OS cells (Fig. 4h). Spatiotemporal studies showed that BmOSER1 is expressed at multiple developmental stages (peaked at L5D1 and wander stage) and tissues (highly expressed in reproductive organs like ovaries and testes) (Supplementary Fig. 10a, b) and that its expression increases with age (Supplementary Fig. 10c).

To understand FOXO regulation of OSER1 in greater detail, we overexpressed FOXO1, FOXO3, FOXO4, and FOXO6 in human U2OS cells following bioinformatic analysis, which predicted the presence of FOXO binding motifs in the promoter region of *OSER1* (Supplementary Table 3). Under basal conditions, direct FOXO target genes, including Catalase (*CAT*) and Superoxide dismutase 2 (*SOD2*), are expressed at a

https://doi.org/10.1038/s41467-024-51542-z

very low level (Fig. 4 d–g). However, exposure to hydrogen peroxide increased the expression of *SOD1* and *OSER1* mRNA (Fig. 4i). These data demonstrate that OSER1 is a target of FOXO and is expressed in the nucleus and induced by oxidative stress.

OSER1 regulates oxidative stress response

To investigate whether OSER1 plays a role in response to oxidative stress, percent survival was measured in *DmOser1* mutant, *DmOser1* overexpressing (OE), and control flies exposed to 20 mM paraquat. The results show lower percent survival in the presence of oxidative stress in *DmOser1* mutant and higher percent survival in *DmOser1*-OE flies than in control flies (Fig. 5a, b). Consistent with this, dihydroethidium (DHE) staining to quantify ROS abundance in the imaginal wing discs suggested lower levels of ROS/oxidative stress in *DmOser1*-OE flies than in control flies (Fig. 5c) mostly due to lower ROS abundance in hinge and wing pouch regions of the wing disc (Fig. 5d).

Fig. 5 | Impact of OSER1 on oxidative stress in *Drosophila* and silkworms. Survival of *DmOser1* mutant (**a**) or overexpression (OE) flies (**b**) fed with the standard diet with 20 mM paraquat. The number of flies in the lifespan experiment: (**a**) yw/DmOser1 ♀ (heterozygous control), $n = 102$; yw/DmOser1mt ♂, $n = 98$; DmOser1mt/DmOser1mt ♀ (homozygous mutant), $n = 100$; DmOser1mt/DmOser1mt ♂, $n = 99$; (**b**) Act-GAL4/+ ♀ (heterozygous control), $n = 74$; Act-GAL4/+ ♂, $n = 65$; Act>DmOser1 ♀ (homozygous overexpression), $n = 74$; Act>DmOser1 ♂, $n = 62$. **c** Control and *DmOser1* overexpression fly larvae imaginal wing discs were stained with DHE (ROS indicator). **d** Quantification of wing disc size and DHE fluorescence intensity in the whole and different regions of wing imaginal discs. Unpaired *t* test, Two-tailed. Whiskers: minima and maxima, Center: median, Bounds of box: 25% and 75% percentile. **e** Transcripts of *DmOser*, *Sod2*, *Cat*, and *GPx* were quantified by qPCR in *Drosophila* larval whole wing discs. $n = 6$ for each group. Unpaired *t* test, Two-tailed. **f** Survival of flies overexpressing *DmOser1* under conditions of starvation. Act-GAL4/+ ♀, $n = 75$; Act-GAL4/+ ♂, $n = 68$; Act>DmOser1 ♀, $n = 75$; Act>DmOser1 ♂, $n = 72$. **g** Survival of *DmOser1* overexpressing flies under heat shock (37 °C). Act-GAL4/+ ♀, $n = 75$; Act-GAL4/+ ♂, $n = 35$; Act>DmOser1 ♀, $n = 75$; Act>DmOser1 ♂, $n = 62$. **h** Survival of *BmOSER1* knockout silkworm larvae under heat shock (37 °C) (mixed sexes). koCtrl, $n = 23$; koBmOSER1, $n = 18$. **i** Expression of *BmOSER1* and *BmCAT* mRNA in adult silkworms treated with 50 mM H_2O_2. Unpaired *t* test, Two-tailed. **j** Expression of *BmOSER1*, *BmSOD1*, *BmCAT*, and *BmGpx* mRNA in BmE cells after treatment with 1 mM H_2O_2. $n = 6$ for each group. Unpaired *t* test, Two-tailed. **k** Staining of silkworm embryonic BmE cells with DCF (dichlorofluorescein) with or without *BmOSER1* overexpression. Unpaired *t* test, Two-tailed. **l** Expression of *BmSOD1*, *BmCAT*, and *BmGpx* mRNA after 1 mM H_2O_2 treatment in the presence or absence of *BmOSER1* overexpression. Scatter plots are presented as mean with SD, and differences between control and treatment groups were analyzed by Unpaired *t*-test, Two-tailed. Survival curves were analyzed using Log-rank (Mantel-Cox) test. n.s., not significant; $^{*}p < 0.05$, $^{**}p < 0.01$, $^{***}p < 0.001$, $^{****}p < 0.0001$. All data points derive from independent cell line lysates, *Drosophila* imaginal wing discs, *Drosophila*, and silkworms. Lifespan experiments were performed at least three times independently with similar observations. Source data are provided as a Source Data file.

Furthermore, *DmOser1*-OE flies expressed lower mRNA levels of antioxidant gene *Sod2* than control flies (Fig. 5e). This aligns with the typical roles of SOD2 that its expression is triggered by oxidative stress[18]; SOD2 overexpressors are more resistant, and its depletions are more vulnerable to oxidative stress in *Drosophila*[31,32]. Female *DmOser1*-OE flies were more resistant to starvation, while male and female *DmOser1*-OE flies were more resistant to heat shock than control flies (Fig. 5f, g). *BmOSER1* knockout silkworm larvae were more sensitive to heat shock than controls (Fig. 5h), and adult male silkworms upregulated *BmOSER1* and *BmSOD1* after heat shock (Supplementary Fig. 8f). When adult silkworms were dosed with 50 mM hydrogen peroxide by injection, transcription of *BmCAT* and *BmOSER1* increased significantly (Fig. 5i) and transcription of *BmOSER1*, *BmSOD1*, *BmCAT*, and glutathione peroxidase 1 (*BmGpx*) increased in BmE cell line treated with hydrogen peroxide (Fig. 5j). When *BmOSER1* was overexpressed in hydrogen peroxide-treated BmE cells, the abundance of ROS declined (Fig. 5k) and expression of *BmSOD1* and *BmCAT* decreased (Fig. 5l). These results indicate that expression of *OSER1* regulates and is regulated by environmental conditions including oxidative stress.

The role of OSER1 in responding to and mitigating oxidative stress was also explored in *Ceoser1* knockdown nematodes. Importantly, *Ceoser1* knockdown nematodes had a shorter lifespan than control nematodes (Fig. 6a and Supplementary Fig. 8g), but lifespan was specifically normalized (lengthened) by N-acetylcysteine (NAC), while control experiments showed that NAC does not extend the lifespan of control nematodes (Fig. 6a). Interestingly, *Ceoser1* overexpression increased the lifespan of nematodes with high levels of ROS after treatment with 4 mM TBHP (Fig. 6b; Supplementary Fig. 2; Supplementary Fig. 8h). Since the *Ceoser1* regulation of lifespan is related to oxidative stress (Fig. 6a), we detected the cellular ROS levels using DCF staining[33] following *Ceoser1* knockdown and found that depletion of *Ceoser1* increased DCF fluorescence (Fig. 6c). This is also confirmed by *Ceoser1* depletion in HyPer expression worms that showed elevated hydrogen peroxide levels (Fig. 6d). Furthermore, when *Ceoser1* was knocked down in nematodes carrying an integrated oxidative stress-inducible GFP tag, GFP fluorescence increased to a level that was further elevated by heat shock (Fig. 6e, f). These results suggest that OSER1 improves resilience and resistance to oxidative stress, which could directly contribute to lifespan extension.

Transcriptomic analyses in *BmOSER1*-overexpressing silkworms and *Ceoser1*-depleted nematodes revealed the potential involvement of OSER1 in mitochondrial biogenesis and other mitochondrial functions (Supplementary Data 5). This was explored by knocking down *Ceoser1* in [*myo-3p::TOM20::RFP(mit)*] and SJ4103 [*myo-3::GFP(mit)*] nematodes with fluorescently labeled mitochondria. Interestingly, fragmented mitochondria were more abundant in *Ceoser1* knockdown nematodes than in control nematodes, and the concentration of intracellular ATP decreased significantly (Fig. 6g–i).

Previous studies showed that in the DAF-2/insulin signaling pathway, *daf-2/InR* (insulin receptor) mutants are more than 100% longer-lived[34]; *age-1/PI3K* mutants are 40% longer-lived[35]; and *daf-16/FOXO* mutants are 12% shorter-lived[36] in *C. elegans*. Here, we show that the expression of *Ceoser1* is lower in *daf-16/FOXO* mutants and higher in *daf-2/InR* mutants (Fig. 6j). In the dietary restriction mimicking mutant *eat-2*[37], *Ceoser1* expression increases (Fig. 6j). Furthermore, in *skn-1/NRF2* gain-of-function nematodes with enhanced detoxification, mitochondrial biogenesis, and longer lifespan[38], *Ceoser1* expression is upregulated (Fig. 6j). However, the expression of *Ceoser1* was not changed in control and *pmk-1/p38* and *glp-1/NOTCH* mutant animals (Fig. 6j, k). In contrast to other known major DAF-16 targets, *Ceoser1* knockdown in *daf-2* mutant nematodes only shortened lifespan by approximately 10% (Fig. 6l). Thus, we conclude that *Ceoser1* is upregulated in pro-longevity *daf-2* and *eat-2* mutants and *skn-1* gain-of-function mutant and downregulated in anti-longevity *daf-16* mutants. This indicates that OSER1 acts downstream of the convergent FOXO node.

OSER1 promotes reproduction

The biological roles of human OSER1 were examined in U2OS cells overexpressing or depleted for OSER1 using a lentiviral expression system. GO analysis of DEGs in OSER1-depleted cells revealed enrichment for genes involved in cellular senescence, cell cycle, senescence-associated secretory phenotype (SASP), oxidative stress-induced senescence, and reproduction and substantial enrichment for genes involved in cell cycle-related pathways in OSER1-OE cells (Fig. 7a–d; Supplementary Data 6; Supplementary Data 7), which is consistent with the nuclear localization of OSER1 in silkworms (Fig. 4c) and U2OS cells (Fig. 4h).

A possible role of OSER1 in reproduction was confirmed by showing that BmOSER1 overexpression increased the fertility of eggs and enhanced male silkworm mating activity, leading to more successful mating events (Fig. 8a–c). Interestingly, depletion of BmOSER1 decreased egg laying (Fig. 8d). In *C. elegans*, the number of progeny was not affected by *Ceoser1* knockdown, but it increased in *Ceoser1*-OE nematodes (Fig. 8e, f).

OSER1 is associated with longevity in humans

Finally, we investigated *OSER1* genetic variants in humans. A total of 49 common single nucleotide polymorphisms (SNPs) in *OSER1*, representing seven independent ($r^2 < 0.1$) LD-based groups of SNPs, fulfilled the applied quality criteria and were detected in 90 + -year-old individuals as well as younger controls (Supplementary Table 4 and 5). The

https://doi.org/10.1038/s41467-024-51542-z

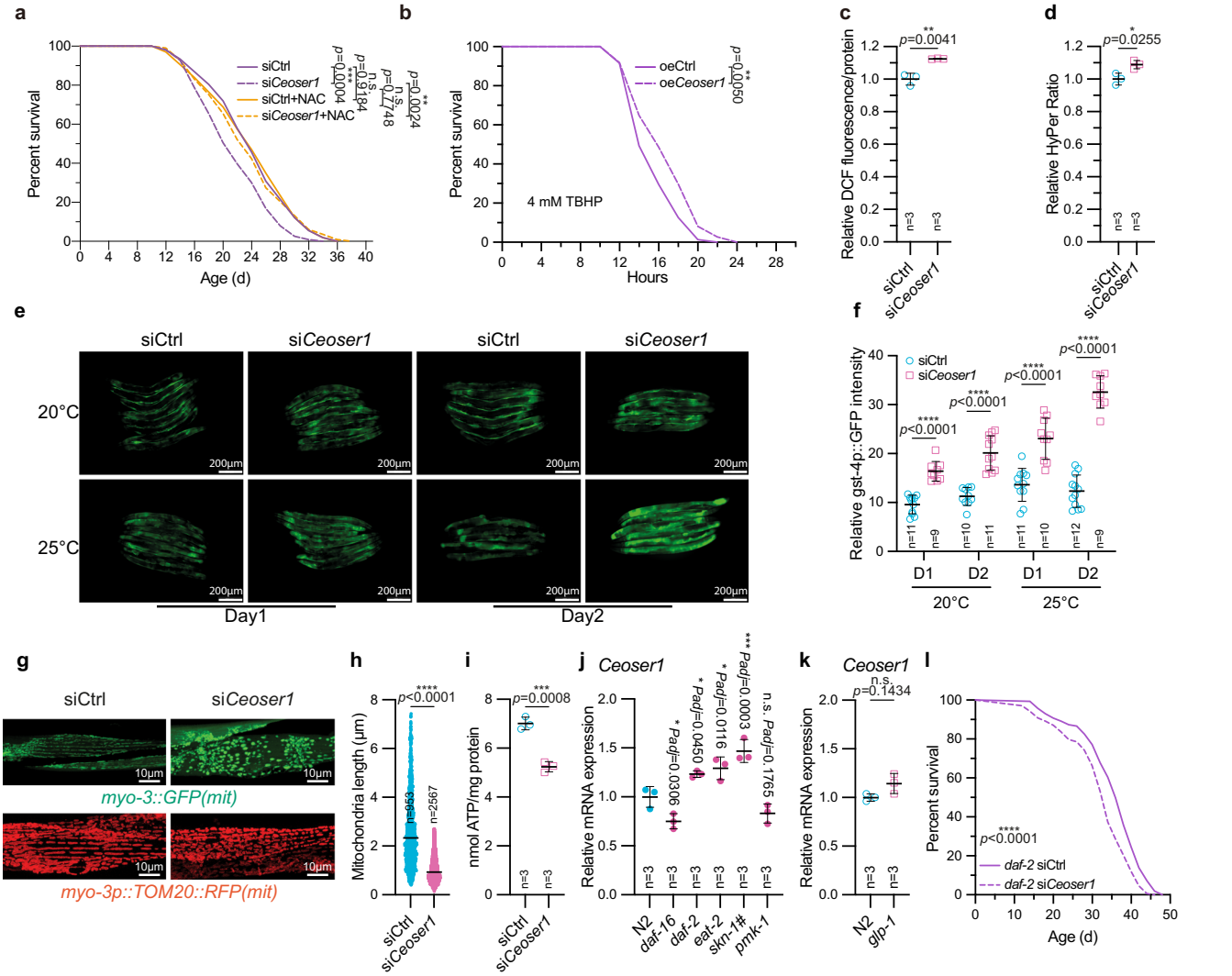

Fig. 6 | OSER1 regulation of lifespan, oxidative stress, and mitochondria in nematodes. a Survival of control and *Ceoser1* knockdown *C. elegans* in the presence or absence of 5 mM NAC (N-acetylcysteine). siCtrl, $n = 107$; siCeoser1, $n = 113$; siCtrl +NAC, $n = 106$; siCeoser1+NAC, $n = 113$. **b** Survival of control and *Ceoser1* over-expressing *C. elegans* stimulated by 4 mM TBHP (tert-Butyl hydroperoxide). oeCtrl, $n = 74$; oeCeoser1, $n = 77$. **c** Quantification of 2′, 7′-dichlorofluorescin diacetate (DCF-DA) fluorescence intensity. Data are presented as mean with SD and analyzed by Unpaired *t*-test, Two-tailed. **d** Quantification of the HyPer fluorescence intensity. Data are presented as mean with SD and analyzed by Unpaired *t*-test, Two-tailed. *Ceoser1* control or knockdown nematodes were imaged for ROS indicator *gst-4p::gfp* at 20 °C or 25 °C on day 1 or day 2 of adulthood (**e**) and quantified in (**f**). Data are presented as mean with SD and analyzed by two-way ANOVA. **g** Representative confocal image of mitochondrial morphology in control and *Ceoser1* knockdown nematode strains with GFP and RFP tagged mitochondria. **h** Quantification of mitochondria length from (**g**). Data are presented as mean with SD and analyzed by Unpaired *t*-test, Two-tailed. **i** ATP levels in control and *Ceoser1* knockdown nematodes. Data are presented as mean with SD and analyzed by Unpaired *t*-test, Two-tailed. Relative expression of *Ceoser1* mRNA in various longevity mutant backgrounds, including *daf-16*, *daf-2*, *eat-2*, *pmk-1*, and an *skn-1* gain-of-function mutant (#) cultured at 20 °C (**j**), and *Ceoser1* mRNA expressions of *glp-1* mutant cultured at 25 °C (**k**). Data in scatter plots are presented as mean with SD and statistically tested by One-way ANOVA (**j**) and Unpaired *t*-test, Two-tailed (**k**). **l** Survival of *daf-2* mutants with normal or low levels of *Ceoser1* expression. All survival curves were plotted and analyzed by Log-rank (Mantel-Cox) test using GraphPad Prism 9. *daf-2* siCtrl, $n = 315$; *daf-2* siCeoser1, $n = 350$. n.s., not significant; $^{*}p < 0.05$, $^{**}p < 0.01$, $^{***}p < 0.001$, $^{****}p < 0.0001$. All data points derive from independent nematodes. Lifespan experiments were performed at least three times independently with similar observations. Source data are provided as a Source Data file.

minor allele dosage for two of 49 SNPs from one independent LD-based group was significantly ($P < 0.0024$) associated with longevity. In addition, the minor allele dosage of five SNPs from another LD-based group was associated with longevity at a nominal significance level ($P < 0.05$) (Supplementary Table 6). No SNPs showed a significant association with age at menopause in long-lived or younger women. However, several nominally significant associations were found (Supplementary Table 7) between higher minor allele dosage and higher age at menopause, especially in long-lived women. In summary, human subject studies support the idea that OSER1 also influences lifespan in humans.

Discussion

Oxidative stress is widely considered a primary driver of aging and age-related diseases[39]. In response to oxidative stress, FOXO proteins upregulate anti-oxidative genes and suppress mitochondrial genes[22,40]. In this study, emerging and well-established animal models of aging were used to identify and characterize the longevity protein OSER1, a highly conserved FOXO-regulated determinant of longevity in silkworms, flies, and nematodes (Fig. 9). The results presented here show that up- or downregulation of OSER1 affects lifespan somewhat more significantly in silkworms and flies than in nematodes. While the molecular basis of this observation is not yet known, we postulate that

https://doi.org/10.1038/s41467-024-51542-z

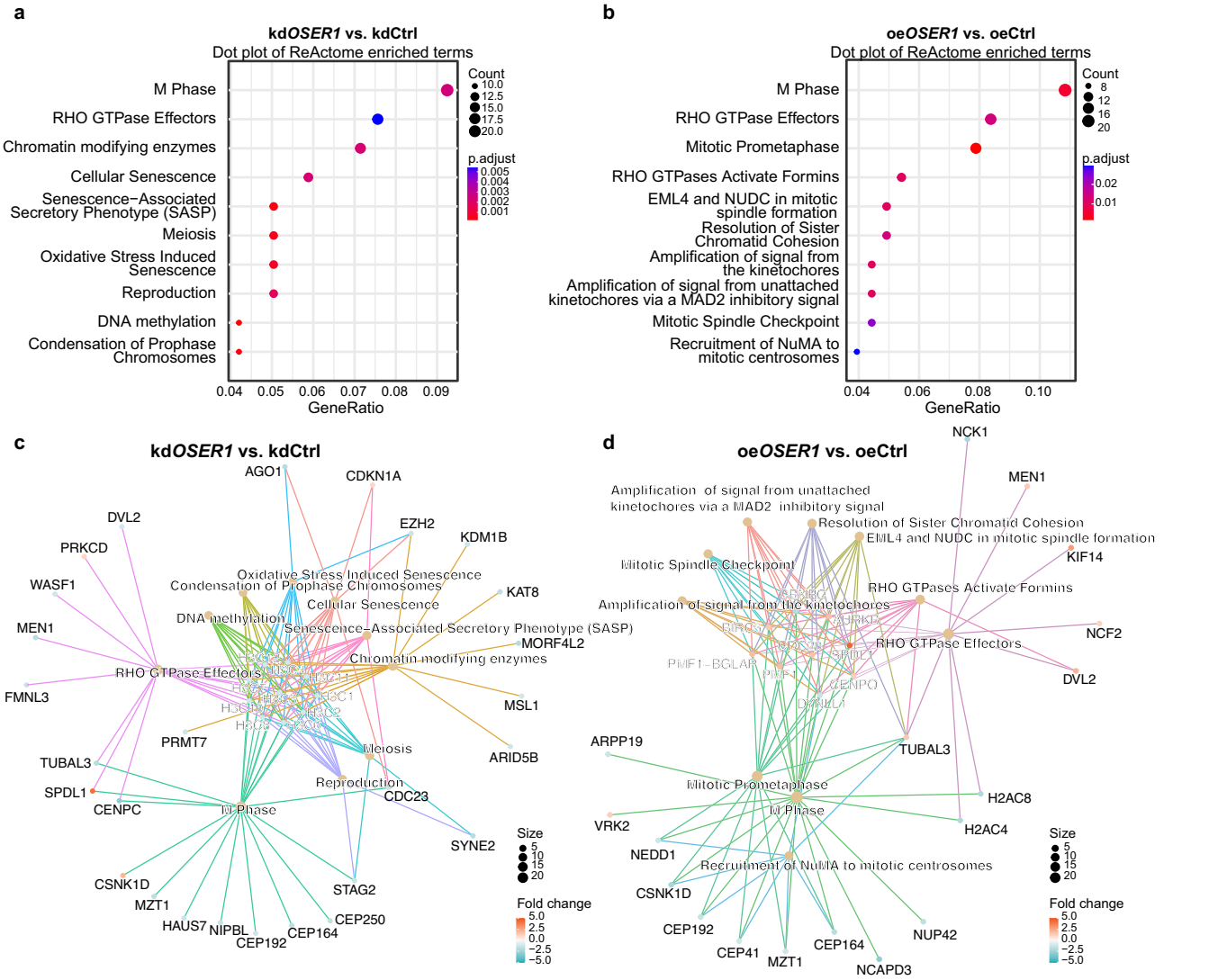

Fig. 7 | OSER1 interaction network by proteomics analyses. a, b KEGG enrichment in U2OS cells with OSER1 knockdown (kd) (**a**) or overexpression (oe) (**b**). The cnetplot of OSER1 knockdown (**c**) and overexpression cells (**d**), based on data summarized in (**a**) and (**b**), respectively. kdCtrl, the lentivirus control U2OS cell line. kdOSER1, the lentivirus-targeted knockdown of OSER1 U2OS cell line. oeCtrl, the U2OS cells transiently transfected with the control plasmid. oeOSER1, the U2OS cells transiently overexpressed with OSER1. All data are available in Supplementary Data 6 and 7.

the physiological function(s) of OSER1 homologs could differ in these diverse species. Transcriptomic data followed by in vivo studies demonstrate that OSER1 provides strong protection against oxidative stress at the organismal and cellular levels, suggesting that it might mitigate oxidative stress downstream of FOXO, similar to SOD2, CAT, and GPX1 in multiple species. In unstressed silkworm and human cells, OSER1 localized to the nucleus, but the network of cytosolic and nuclear proteins that mediates the biological effects of OSER1 remains poorly understood.

Heat stress can increase the lifespan of yeast[41] and *C. elegans*[42], which could potentially reflect and be dependent on increased expression of heat shock factor (HSF-1)[43]. HSF1 and FOXO cooperate to activate the expression of small heat-shock proteins to extend lifespan[44]. Downregulation of DAF-16/FOXO and HSF-1 activity has been linked to a shorter lifespan in *C. elegans* with glucose supplementation[45]. Heat stress stimulates the production of ROS and the expression of both MnSOD[46] and BmOSER1 (Supplementary Fig. 8f). A recent study in zebrafish also demonstrated a correlation of heat shock with increased expression of OSER1 and ROMO1[47]. Nevertheless, the mechanism by which OSER1 confers thermotolerance remains unclear.

In summary, the current study presents strong evidence that OSER1 increases resilience and resistance to oxidative stress, heat shock, and other types of cellular stress, while at the same time causing an apparent increase in lifespan in multiple species. Finally, we emphasize the need for further research on the biological roles and mechanism of action of the longevity protein OSER1.

Methods

Cell culture and transcriptomics

Cell culture. *Bombyx mori* BmN-SWU1 cells were cultured in TC-100 insect medium[48], and BmE cells were cultured in Grace insect medium[49]. *Spodoptera frugiperda* Sf9 cells were cultured in Sf-900™ III SFM insect medium (Thermo Fisher Scientific, USA)[50]. These cell cultures were grown at 27 °C under sterile conditions, as previously reported[48,50].

Transcriptomics. Cell lines pIZ/V5-FoxO^{CA} and pIZ/V5-siFoxO were grown under selection by zeocin for 48 h post-transfection. For each sample, cells from three independent cell culture flasks were pooled. Total RNA was extracted using Trizol Reagent (Invitrogen, USA) according to the manufacturer's instructions. A differential gene

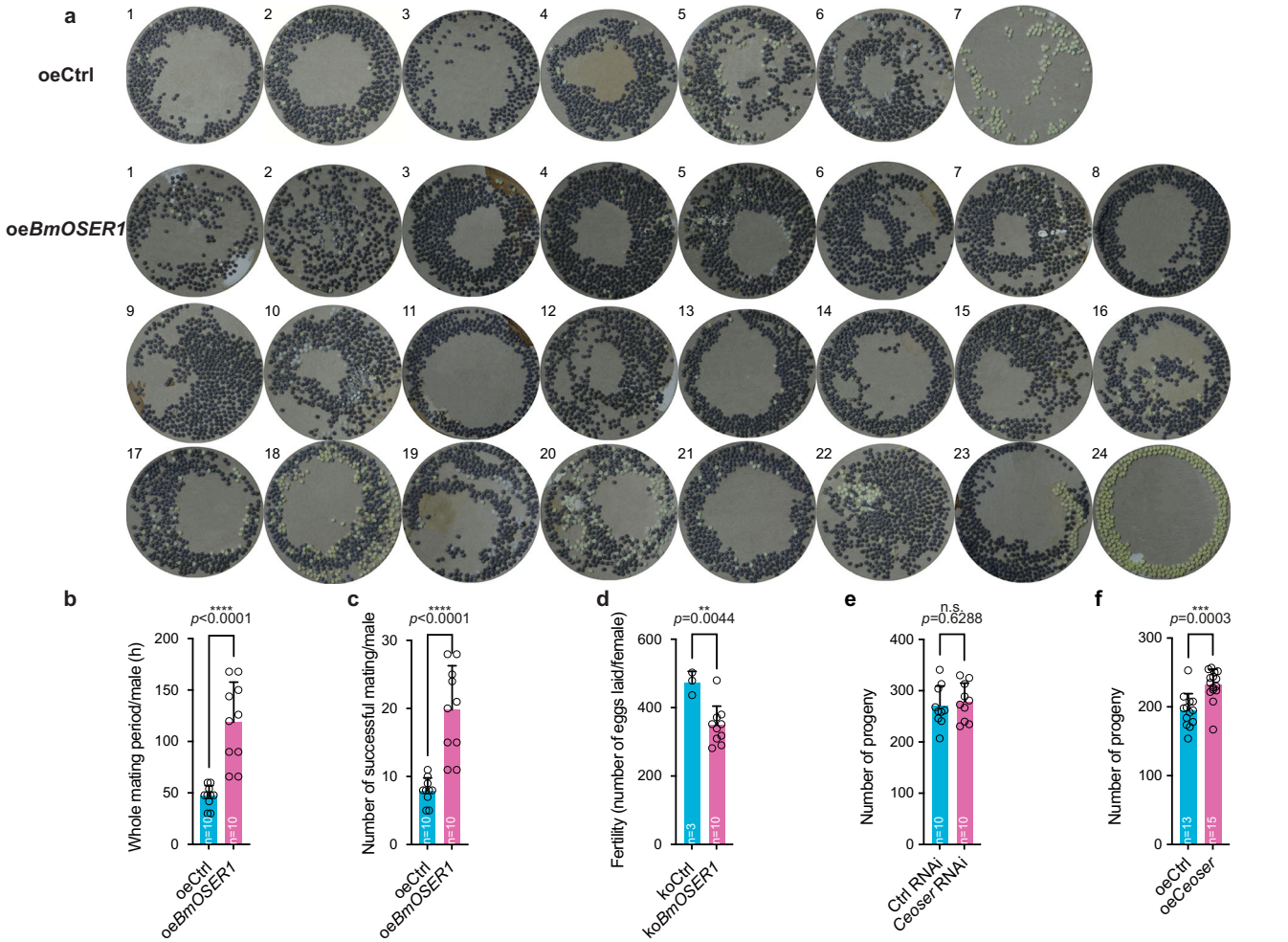

Fig. 8 | Effects of *BmOSER1* and *Ceoser1* on reproduction. a Representative images of eggs laid by wildtype (oeCtrl) and *BmOSER1* overexpression (oeBmOSER1) silkworms. As shown, one male silkworm mates with 6 females in the wildtype Dazao and produces hatchable eggs, while in *BmOSER1* overexpression silkworms, one male mates with 23 females that laid hatchable eggs. **b** Duration of the entire fertile mating period between male and female adult silkworms. **c** Number of successful matings per male adult silkworms. **d** The number of eggs laid per female adult silkworms in wildtype and *BmOSER1* knockout. **e**–**f** The total brood sizes of *Ceoser1* RNAi (*Ceoser1* RNAi) (**e**) and overexpression (oeCeoser) (**f**) throughout life. Data in all scatter plots are presented as mean with SD and analyzed by Unpaired *t*-test, Two-tailed. n.s., not significant; $^{**}p < 0.01$, $^{***}p < 0.001$, $^{****}p < 0.0001$. All data points derive from independent silkworms or nematodes. Source data are provided as a Source Data file.

expression library was constructed and analyzed by GENE DENOVO Corporation (Guangzhou, China). *Bombyx mori* BmFoxO Raw sequence reads data can be found at PRJNA943622 [https://www.ncbi.nlm.nih.gov/bioproject/PRJNA943622/#. RNA-Seq data for Control (Accession No. SRX20534814), BmFoxO-RNAi (Accession No. SRX20534813), and FoxO^{CA}-OE (Accession No. SRX20534812).

Analysis of differentially-expressed genes (DEGs). The Omicshare website tool (https://www.omicshare.com/) was used to identify differentially-expressed genes across samples or groups. We identified genes with a fold-change ≥2 and a false discovery rate (FDR) threshold ≤0.05. DEGs were then analyzed for enrichment of GO functions and KEGG pathways using the Omicshare website tool.

Phylogenetic analysis

Each OSER1 protein sequence was downloaded on the NCBI website, and the Muscle software was employed to perform multiple sequence alignment[51]. Bayesian inferences were performed using MrBayes v3.2.7 to calculate the tree statistics, including the mean and variance of split or clade frequencies and branch rates[52,53]. The Java-jarprotest-3.3.jar was employed to detect the most suitable model to reconstruct the phylogenetic tree[54]. The "MCMC" command was used for running the process[54,55].

Dual-luciferase reporter assay

The upstream regulatory regions (−1500 bp to 0 bp) of the *oser1* gene from the silkworm wildtype Dazao strain were amplified using primers PGL-F and PGL-R. The PCR products were cloned into the PGL3-Basic vector (Promega). The PGL3-*oser1*-luciferase recombinant plasmid and the FoxO^{CA} overexpression plasmid were cotransferred with the reference plasmid (containing Renilla luciferase gene driven by *Ie1* promoter) separately into silkworm BmN-SWU1 cells and *Spodoptera frugiperda* Sf9 cells using X-tremeGENE HP DNA Transfection Reagent (Roche, USA) was used according to the manufacturer's instructions. At 72 h post-transfection, cells were collected for luciferase assays.

Quantitative real-time PCR (RT-qPCR)

Silkworm tissues were collected to quantify *BmOSER1* mRNA at different developmental stages, and total RNA was isolated using TRIzol (Invitrogen) according to the manufacturer's instructions. Reverse transcription and quantitative real-time PCR (RT-qPCR) were performed as previously described[56]. The primers used for RT-qPCR are

https://doi.org/10.1038/s41467-024-51542-z

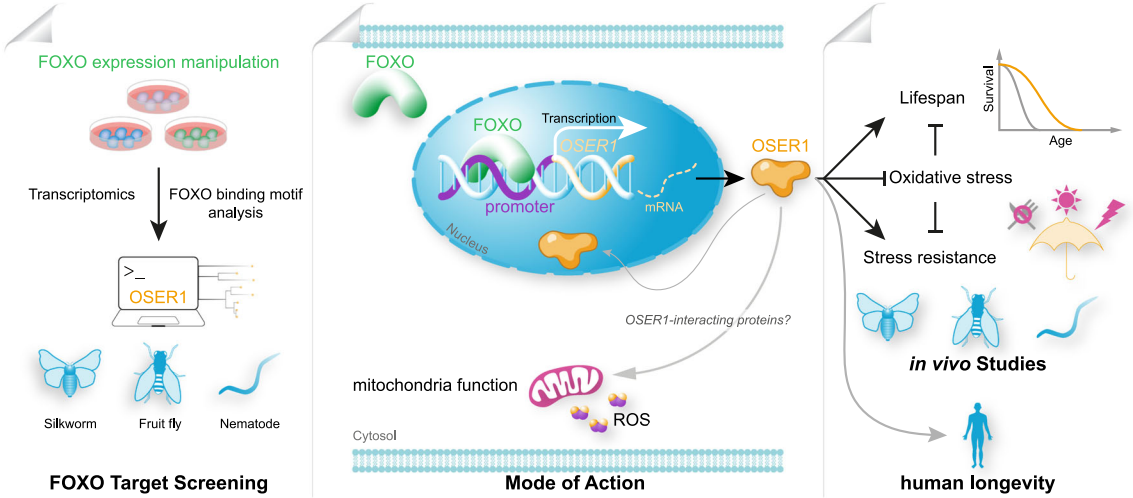

Fig. 9 | Schematic representation of workflow and model. Transcriptomic analyses of FOXO transcriptional targets in silkworms identified an evolutionarily conserved FOXO direct target OSER1. Mechanistically, FOXO protein binds to the promoter of *OSER1* to activate its transcription. OSER1 expression is essential for normal mitochondrial morphology and functions, as well as low levels of reactive oxygen species (ROS), possibly via interacting with other as yet unidentified proteins. The in vivo studies showed the critical roles of OSER1 in longevity and stress resistance (especially oxidative stress response) in silkworms, flies, and nematodes. Interestingly, human subject studies support the idea that OSER1 also influences the human lifespan. This figure was created by BioMedVisual.com.

listed in Supplementary Table 8. *sw22934/ BmeIF4A* was used as a previously-validated RT-qPCR reference gene for the silkworm[57]. As shown in the Supplementary data, our RT-qPCR experiments follow almost all the criteria of the MIQE guidelines[58].

Vector construction

For gene overexpression, selected promoter, ORF, and poly-A regions were inserted into recipient vectors using standard cloning procedures (Supplementary Fig. 2). For knockdown constructs, the interference fragment for selected target genes was inserted into commercially-available vectors according to standard procedures. To express the product with the interference effect (Supplementary Fig. 2).

Prokaryotic protein expression

The pET-32a (+) vector with His tag was used to express the BmFoxO protein in *E. coli*, and a histidine affinity column (HisTrap HP) was used for protein purification. Recombinant protein-containing culture supernatant was filtered using a 0.22 μm membrane prior to affinity chromatography. Bound protein was washed using 10, 20, and 30 column volumes of binding buffer and was eluted with 20 column volumes of elution buffer containing 80 mM Imidazole. Eluted protein was collected in separate tubes, and the column was washed with 5 column volumes of Elution Buffer (100 mM Imidazole) to elute residual protein. Finally, the column was washed with 10 column volumes of Binding Buffer (40 mM Imidazole), 5 column volumes of 20% ethanol, and the column was stored at 4 °C. In general, a flow rate of 1 mL/min was maintained.

Electrophoretic mobility shift assay (EMSA)

The 3000 bp genomic sequence upstream of the *BmOSER1* start codon was input to JASPAR for the prediction of putative transcription factor (TF) binding sites. For the EMSA assay, the labeled probe and competitor probe were designed according to the binding motif with or without biotin, respectively. Probes were diluted to 10 μM and annealed to respective complementary probes. 0.5×TBE was used as the electrophoresis and transfer buffer, and protein transfer was performed for 8 min. Then, the 254 nm UV light was used for cross-linking for 15 min. Biotin-labeled probes were detected by chemiluminescence.

Confocal microscopy

BmN-SWU1 cells were plated in a 24-well plate and transfected with 500 ng of the expression vector (pIZ/V5-His, pIZ/V5-His-BmFoxO, pIZ/V5-His-BmFoxO^{CA}). At 96 h post-transfection, cells were fixed with 4% paraformaldehyde in PBS for 15 min at room temperature. Fixed cells were permeabilized in 0.1% Triton X-100 in PBS for 10 min. Cells were blocked with 10% normal goat serum in PBS for 1 h at 37 °C, followed by incubation with anti-His antibody (1:200, Beyotime) for 1 h at 37 °C. Cells were stained with anti-mouse Alexa 555 (1:500) antibody for 1 h and mounted with 0.1 g/ml DAPI (Sigma, USA) for observation under a confocal microscope (Olympus, Japan). BmN-SWU1 cells were plated in a 24-well plate and transfected with 500 ng of the expression vector (pIZ/V5-His-BmOSER1-DsRed2). At 48 h post-transfection, cells were fixed with 4% paraformaldehyde in PBS for 10 min at room temperature. Fixed cells were permeabilized in 0.1% Triton X-100 in PBS for 10 min and stained with DAPI (Beyotime) for imaging under a confocal microscope (Olympus, Japan).

Lifespan assay

Silkworm wildtype Dazao strain was reared under standard conditions (25 °C, in approximately 75% relative humidity with a 12 L/12D photoperiod) with clean and fresh mulberry leaves during the whole larval stage in the Silkworm Gene Bank at Southwest University. Survival was monitored every 3 h. Silkworms that did not move when gently prodded were marked as dead and recorded. Maximum lifespan refers to the upper 10% of the distribution of lifespan.

Transgene overexpression and gene interference in individual *BmOSER1* silkworms

BmOSER1 was overexpressed or subject to RNAi knockdown in wild-type silkworms (Dazao strain). The *BmOSER1* overexpression plasmid was constructed using a 3p3×piggyBac-EGFP basic vector by inserting the IE2-*oser1* (ORF)-SV40 expression box. The *oser1* overexpression plasmid was mixed with the A3 helper vector and injected into silkworm eggs within 2 h after laying. EGFP fluorescence in the silkworm compound eye was used as a marker for transgene-expressing individual worms. Samples were collected separately for RT-qPCR analysis at larval and adult stages.

The *BmOSER1*-dsRNA fragment was obtained by PCR amplification from the full-length cDNA with a pair of primers containing the T7

RNA polymerase binding site (14). The *BmOSER1*-dsRNA (ds*BmOSER1*) and the red fluorescent protein gene dsRNA (dsRed) were synthesized using the T7 RiboMAX Express RNAi kit (Promega, USA) according to manufacturer's instructions. The dsRNA (ds*BmOSER1* and dsRed, 120 μg) was injected into hemolymph through the penultimate spiracle on the 10th day after pupation. Samples were collected for RT-qPCR analysis 12 and 24 h after molting. Lifespan analysis was conducted as described.

Stress assay

Cell and individual silkworm exposure to oxidative stress. Cells were distributed in a 12-well cell culture plate and grown to approximately 80% maximum cell density, prior to transfection with vector control, pIZ/V5, or pIZ/V5-*BmOSER1* overexpression plasmid. After 48 h, cells were washed gently with PBS, and exposed to fresh culture medium containing 600 μl 1 mM H_2O_2 (Sigma, USA) per well; after 1 h, cells were collected, treated with lysis solution and then stored at −20 °C. For the treatment of individual silkworms, injection devices, syringes, and capillaries were prepared. Each worm was injected with 10 μl H_2O_2 by the needle through the intersegment membrane on day 1 after the moth eclosion in male and female individuals. The control group was injected with the same volume of 1 × PBS solution. These materials were used for checking the ROS content by the Reactive Oxygen Species (ROS) Assay Kit (Comin, China) or for detection of gene expression levels by the microRNA extraction kit (Omega, USA).

ROS detection. DCFH-DA was diluted into serum-free medium at a ratio of 1:1000 and added to cells. Cells were incubated for 20 min at 27 °C and, and then washed 3x with serum-free medium. Cells were imaged and fluorescence was detected on a microplate reader using 488 nm excitation and 525 nm emission.

Thermotolerance. Developmentally consistent female and male individuals were selected on day 1 after eclosion and incubated at 37 °C or 25 °C. Survival was measured as described.

Drosophila melanogaster techniques

Lifespan assay. The *DmOser1* mutant stock was obtained from the Bloomington Drosophila Stock Center (#21830), and the overexpression stock was from FlyORF (#F002710). The *yw* and *w1118* were reared as previously described[59]. For lifespan assay, newly emerged female and male flies were separated, and healthy flies with similar body sizes were selected. For each group, 4 vials, and 25 flies/vial were used at the start of survival measurement. Food was changed every three days, and the number of dead flies was recorded. Control and *DmOser1* mutant flies were incubated at 25 °C with controlled humidity. For mild *DmOser1* overexpression, flies were also incubated at 25 °C, while flies with higher *DmOser1* overexpression and control flies were incubated at 29 °C.

Stress assay. For oxidative stress assay, flies were collected in vials containing standard food containing 20 mM paraquat. For each group, 4 vials (25 flies/vial) were incubated at 25 °C with controlled humidity. Survival was monitored every three hours. For the starvation assay, experimental conditions were the same, except standard food was replaced with 1% agar and survival was monitored every hour. For the thermotolerance assay, flies were placed in vials containing standard food and incubated at 25 °C or 29 °C.

RT-qPCR. RNA extraction and RT-qPCR for adult *Drosophila* were performed as previously described[59]. For larval *Drosophila*: wing discs were dissected from 25 to 30 L3 wandering *Drosophila* larvae, and total RNA was extracted according to the Trizol protocol (Life Technologies, #15596026). DNase treatment was performed on RNA samples with RQ1 DNase I (Promega, #M6101), and cDNA was prepared using the SuperScript III Reverse Transcriptase kit (Life Technologies, #18080-044). RT-qPCR was run on the QuantStudio 6 Flex Real-Time PCR machine (Applied Biosystems) using the 5x HOT FIREpol EvaGreen qPCR Mix Plus (Solis BiodDyne, #08-24-00001). DNA sequences of all primers are shown in Supplementary Table 8.

Dihydroethidium (DHE) staining. L3 wandering larvae were dissected in Schneider's *Drosophila* media (Gibco, #11720). Samples were then stained with DHE (Invitrogen, #D11347) diluted in Schneider's media for 5 to 7 min at room temperature under conditions of darkness. All subsequent steps were performed at room temperature in the dark. DHE-containing medium was removed, discs were washed 3 times for 5 min each with Schneider's media and then incubated in 7% formaldehyde / PBS for 5 min. Samples were washed once for 5 min with PBS and mounted for imaging in 90% glycerol / PBS /0.05% N-propyl gallate. Stained samples were imaged with a Leica SP8 confocal laser-scanning microscope.

Caenorhabditis elegans techniques

***C. elegans* strains and maintenance.** *C. elegans* were cultured at 20 °C on a standard nematode growth medium (NGM) seeded with E. coli OP50-[60] unless stated otherwise. The wild-type N2 Bristol, CL2166[*gst-4p::gfp*], KU25[*pmk-1(km25)*], SPC167[*skn-1(lax120)*], DR1572[*daf-2(e1368)*], CB4037[*glp-1(e2141)*], DA465[*eat-2(ad465)*], CF1038[*daf-16(mu86)*] strains were provided by the Caenorhabditis Genome Center. The muscle mitochondria-targeted fluorescent protein strain [*myo-3p::TOM20::RFP(mit)*] was provided by Dr. Shanshan Pang and SJ4103 [*myo-3::GFP(mit)*] was provided by Dr. Shiqing Cai. FYD19[*eft-3p::F02E9.5a*] transgenic worms were constructed by cloning the promoter of *eft-3* and full-length *F02E9.5a*(*Ceoser1*) genomic DNA into pPD95_79 plasmid followed by standard microinjection.

RNA interference treatment. For the RNAi experiment, HT115 bacteria containing specific dsRNA-expression plasmids (Ahringer library)[61] were cultured overnight at 37 °C in LB containing 100 μg/mL carbenicillin and seeded on NGM plates containing 5 mM IPTG. RNAi Plasmid L4440 (2790 bp, Addgene, #1654) was used as a control in the RNAi experiment. RNAi was induced at 25 °C for 24 h after seeding. Then, synchronized L1 worms were added to RNAi plates to knock down the indicated genes. Primer sequences are listed in Supplementary Table 8.

Vector construction for *Ceoser1* overexpression. The pPD95_79 Plasmid was a gift from Andrew Fire (Addgene, #1496) and was employed as the basic recipient vector. The eft-3 promoter (600 bp) was inserted from Hind III to Xba I, and *F02E9.5a* genomic DNA (1147 bp) was inserted from Xba I to Sma I. The pPD95_79 basic plasmid was set as control.

RT-qPCR. RT-qPCR was performed as previously described[62]. Briefly, day1 worms were collected, washed in M9 buffer, and then homogenized in TRIzol reagent (Life Technologies). RNA was extracted according to the manufacturer's protocol. DNA contamination was digested with DNase I (Thermo Fisher Scientific), and RNA was subsequently reverse-transcribed to cDNA using the RevertAid First Strand cDNA Synthesis Kit (Thermo Fisher Scientific). Quantitative PCR was performed using SYBR Green (Bio-Rad). The expression of *snb-1* was used to normalize samples. Primer sequences are listed in Supplementary Table 8.

Fluorescence microscopy. Microscopic imaging was performed as previously described[33]. Briefly, unless otherwise indicated, day 1 adult worms were collected, washed in M9 buffer, and then paralyzed with 1 mM levamisole. Fluorescence microscopic images were taken after mounting on 2% agarose pad slides.

Lifespan assay. Lifespan assays were performed as previously described[63] with modifications. Briefly, synchronized L1 worms were added to NGM plates seeded with different *E. coli* strains. Worms were transferred every day during the reproductive period. Worms that died of vulva burst, bagging, or crawling off the plates were censored. For NAC treatment, concentrated NAC (Sigma) was added to NGM plates at a final concentration of 5 mM NAC.

ROS measurement. ROS measurement for hydrogen peroxide assays was performed as previously described[64]. Briefly, the day 2 adult HyPer expression worms jrIs1[Prpl-17::HyPer] were mounted on slides, and excited with GFP and CFP channels to measure the oxidized and reduced HyPer, respectively. Fluorescence microscopic images were then taken, and fluorescent density was measured using ImageJ software. The ratio of oxidized to reduced HyPer intensity was calculated as the hydrogen peroxide levels. ROS measurement assays using DCF-DA (Sigma) were performed as described previously[33]. Briefly, approximately 1000 adult worms (day 2) were collected, washed three times in M9 buffer, then homogenized in PBST (PBS, 0.1% Tween 20), and subsequently centrifuged twice at 13,000 rpm at 4 °C for 10 min. The supernatant was used for protein concentration determination (bicinchoninic acid (BCA) assay) and ROS levels measurement. The supernatant containing 20 μg of protein was pre-incubated with 200 μM of DCF-DA in 100 μl of PBS at 37 °C for 1 h. Fluorescent intensity was then measured at the excitation wavelength of 485 nm and the emission wavelength of 530 nm every 10 min for 1 h. Fluorescent intensity was normalized, and background fluorescence was subtracted.

ATP measurement. ATP levels were measured as previously described[64]. In brief, about 300 adult worms (day 2) were collected and washed three times in M9 buffer. The worms were then homogenized by boiling for 20 min and centrifuged at 13,000 rpm at 4 °C. The supernatant was used for ATP concentration determination according to the manufacturer's protocol (ENLITEN ATP Assay; Promega). The protein content in the supernatant was determined by employing a BCA assay to normalize the ATP levels.

Silkworm and *C. elegans* OSER1 transcriptomics. Eggs of wild-type Dazao silkworm were injected into a mixture of piggyBac-BmOSER1 overexpression plasmid and pHA3PIG A3-helper plasmid. After culture and screening, the *BmOSER1* overexpression strain was successfully constructed. The male adults on the first day of the adult stage ($n = 3$) from wild-type Dazao and *BmOSER1* overexpression strains were sampled. Synchronized L1 worms were added to *Ceoser1* RNAi and control plates separately and cultured to day 1 of adulthood at 20 °C. Total RNA was extracted using the TRIzol reagent kit (Invitrogen, Carlsbad, CA, USA), and the extraction procedure was performed according to the manufacturer's protocol. RNA quality was assessed using an Agilent 2100 Bioanalyzer (Agilent Technologies, Palo Alto, CA, USA) and checked using RNase-free agarose gel electrophoresis. The sequencing Libraries were thereafter constructed and sequenced using an Illumina Novaseq 6000 150PE by Gene Denovo Biotechnology Co., Ltd. (Guangzhou, China). The input data for differential gene expression analysis were the read counts obtained from gene expression level analysis. The analysis was performed using the DESeq2 software, which was divided into three main parts, firstly, normalization of read counts. then calculation of p-values based on the model; Finally, multiple hypothesis testing correction is performed using Benjamini-Hochberg method to obtain the FDR values (False Discovery Rate). Based on the results of the differential analysis, genes between the control group and the treated group with the parameter of the false discovery rate (FDR) < 0.05 and absolute fold change (FC) ≥ 2 were considered differentially expressed genes (DEGs). Significance test of enrichment analysis was performed by calculating the corresponding q-value which is obtained by multiple testing of the p-value. It was considered that the gene had been significantly enriched when the *q*-value was <0.05. The raw sequencing data generated from this study were deposited in NCBI under the BioProject ID PRJNA978397 and PRJNA978499. The identified DEGs were subsequently subjected to enrichment analysis of GO and KEGG with the OmicShare website tool. The various significantly enriched GO terms and KEGG pathways were defined with a hypergeometric test (corrected p-value < 0.05).

Human cells

Cell culture. Human U2OS osteosarcoma cells were cultured in DMEM (Gibco, #31966021) supplemented with 10% FBS and 1% Penicillin-Streptomycin (Gibco, #15140122). Cells were cultured in a 37 °C incubator with 5% CO_2.

RT-qPCR. 5x HOT FIREPol® EvaGreen® qPCR Mix Plus (ROX) (Solis BioDyne, #08-36-00020) was used for determining gene expression on the StepOne™ Real-Time PCR System. Experiments were performed following the manufacturer's instructions. RT-qPCR primers were included in Supplementary Table 8.

Transient transfection of human pCS2, FOXO1, FOXO3, FOXO4, and FOXO6. U2OS cells were seeded to 6-well plates the day before transfection. The next day, pCS2, FOXO1, FOXO3, FOXO4, and FOXO6 were transfected into U2OS cells at 80% confluency. These plasmids are generously provided by Stefan Koch[65]. 1 ug plasmid was transfected to each well of 6-well plates by using Polyjet transfection reagent (SignaGen, #SL100688). RNA samples were collected after 72 h to measure gene expression.

Immunofluorescence and microscopy. U2OS cells were seeded on the coverslips of the 24-well plate. The next day, cells were washed with PBS once and then fixed by adding 4% paraformaldehyde (Sant Cruz, #30525-89-4) for 15 min at room temperature. Then, cells were rinsed three times in PBS for 5 min each. Afterward, cells were blocked by blocking&permeabilization buffer (5% goat serum +0.2% Triton-100 in PBS) for 60 min at room temperature first and then incubated with blocking&permeabilization buffer diluted OSER1 antibody (Merck, # HPA045125) overnight at 4 °C. The next day, coverslips were rinsed with PBS three times for 5 min each, and the coverslips were incubated with PBS-diluted Goat-anti-Rabbit secondary antibody (ThermoFisher, #A-11011) for 2 h at room temperature. Then coverslips were rinsed with PBS three times for 5 min each after secondary antibody incubation and then stained with PBS diluted Hoechst (ThermoFisher, #62249) (ThermoFisher, #P36965) for 5 min and washed with PBS twice for 5 min each. Afterward, the coverslips were mounted with a Prolong-gold mounting medium for imaging by confocal laser scanning microscope LSM710 (Zeiss).

Lentivirus packaging and infection. The lentiviruses were packaged in HEK293T cells together with packaging vectors (plasmid (9 μg), pMDLg/pRRE (4.5 μg), pRSV-Rev (4.5 μg), and pMD2.G (4.5 μg) using 45 μg 1 ug/uL PEI (polyethylenimine, transfection reagent). Lentivirus-containing media were collected 48 h later and filtered through a 0.45 μm filter to remove the cell debris and used to infect control and AD fibroblasts. After 8 h infection for lentivirus, the medium was changed to the normal culture medium.

Mass spectrometry proteomics analysis. Cells were washed twice with cold phosphate-buffered saline (1 × PBS) and then rapidly lysed, and cysteines were reduced and alkylated in a single step. Briefly, boiling 6 M guanidine hydrochloride (Gnd-HCl) containing 10 mM chloroacetamide and 5 mM tris(2-carboxyethyl)phosphine was added directly to the cells. Lysis buffer containing cells was boiled for an additional 10 min at 99 °C, followed by sonication for 2 min. Samples

are diluted using 50 mM ammonium bicarbonate to approximately 0.3 M GdnCl final concentration and an aliquot containing 12 μg protein was digested with Trypsin (Sigma-Aldrich) (0.5 μg/μl) for 18 h at pH 8.5, 37 °C.

After spinning down for 5 min at 17,000 × g, 500 ng peptides were immobilized and purified on EvoTips. All samples were analyzed on an Orbitrap Exploris 480 mass spectrometer coupled with an Evosep One system using an in-house packed 15 cm, 150 μm i.d. capillary column with 1.9 μm Reprosil-Pur C18 beads (Dr. Maisch, Ammerbuch, Germany) using the pre-programmed gradients (30 samples per day) in data-independent acquisition (DIA) mode as described before[66]. Briefly, full MS resolutions were set to 120,000 at m/z 200 and full MS AGC target was 300% with an IT of 45 ms. Mass range was set to 350–1400. AGC target value for fragment spectra was set at 1000%. 49 windows of 13.7 Da were used with an overlap of 1 Da. Resolution was set to 15,000 and ion injection time to 22 ms. Normalized collision energy was set at 27%. All data were acquired in profile mode using positive polarity and peptide match was set to off, and isotope exclusion was on. All samples were acquired in four replicates ($n = 4$) and a total number of 24 samples were analyzed including four control samples.

All DIA raw files were processed with Spectronaut (v15, Biognosys, Zurich, Switzerland) in DirectDIA mode using human Uniprot Reference Proteome without isoforms (21,074 entries). We used standard settings in Spectronaut for peptide identification, protein quantification, and determination of significantly regulated proteins. Briefly, cysteine carbamylation was set as a fixed modification, whereas methionine oxidation and protein N-terminal acetylation were set as variable modifications. Precursor filtering was set as Q value, and cross-run normalization was checked. The results of the differential abundance testing were exported from Candidates table node. The table is filtered by a q-value (Benjamini-Hochberg multiple testing corrected p-value) of 0.05 and an absolute log2 ratio of 0.58. Functional enrichments were conducted with in-house written R-scripts using clusterProfiler. The mass spectrometry proteomics data have been deposited to the ProteomeXchange Consortium via the PRIDE partner repository with the dataset identifier PXD036579.

Human studies

The study is registered in SDU's internal list (notification no. 11.648) and complies with the rules in the General Data Protection Regulation. Written informed consent was obtained from all participants. The collection and use of biological material and survey and registry information were approved by the Regional Committees on Health Research Ethics for Southern Denmark.

Samples. Long-lived individuals (LLIs), *i.e.*, individuals >90 years old, were drawn from six nationwide surveys collected at the University of Southern Denmark; the Study of Danish Old Sibs (DOS), the 1905 birth cohort study, the 1910 birth cohort study, the 1911-12 birth cohort study, the 1915 birth cohort study, and the Longitudinal Study of Ageing Danish Twins (LSADT). The younger controls were drawn from the Middle-Aged Danish Twins (MADT) study. Briefly, DOS was initiated in 2004 and included families in which at least two siblings were ≥90 years of age at intake. The 1905, 1910, and 1915 birth cohort studies are prospective follow-up studies initiated in 1998, 2010, and 2010, when participants were 92-93, 100, and 95 years of age, respectively[67]. The 1911-1912 birth cohort study consists of individuals reaching the age of 100 years in the period from May 2011 to July 2012[68], and LSADT was initiated in 1995 and included Danish twins ≥70 years of age[69]. The younger controls were obtained from MADT that was initiated in 1998 and included twins randomly chosen from the birth years 1931–1952[69]. From DOS and LSADT, one individual from each sib-ship or twin pair was randomly selected among participants that had reached an age of at least 91 years for DOS and 90 years for LSADT. From the 1905 and 1915 birth cohort studies, participants were selected among individuals reaching an age of at least 96 years. From MADT, one individual from each monozygotic twin pair was randomly selected. From dizygotic twin pairs, both twins were included.

DNA was extracted from whole blood using standard methods[70], or from filter cards using the Extract-N-Amp Blood PCR Kit (Sigma Aldrich, St. Louis, MO, USA) followed by amplification using the GenomePlex Complete Whole Genome Amplification (WGA) Kit (Sigma Aldrich, St. Louis, MO, USA).

Genotype data. The included individuals were genotyped as part of one of two data sets. In data set 1, individuals from DOS, 1905, 1910, 1911-12, and 1915 birth cohort studies, and LSADT were genotyped using the Illumina Human OmniExpress Array (Illumina San Diego, CA, USA). Pre-imputation quality control included filtering SNPs on genotype call rate <95%, HWE $P < 10^{-4}$, and MAF = 1%, and individuals on sample call rate <95%, relatedness, and gender mismatch. Pre-phasing and imputation to the 1000 Genomes phase I v.3 reference panel were performed using IMPUTE2 version 2.3.2[71]. In data set 2, individuals from LSADT and MADT were genotyped using the Illumina Infinium PsychArray (Illumina San Diego, CA, USA). Pre-imputation quality control included filtering SNPs on genotype call rate <98%, HWE $P < 10^{-6}$, and MAF = 0, and individuals on sample call rate <99%, relatedness, and gender mismatch. Pre-phasing and imputation to the 1000 Genomes phase 3 reference panel were performed using IMPUTE2 version 2.3.2[71]. After imputation, genotype probabilities were converted to hard-called genotypes in Plink[72] using a cut-off of 90%, meaning that only genotypes with a probability of more than 90% were called. Variants with no genotype probabilities above 90% were set to missing.

Data on single nucleotide polymorphisms (SNPs) in the *OSER1* gene, including 5000 bp upstream and 1000 bp downstream to cover regulatory regions (total region; chr20:42,823,581-42,844,546), was extracted from the hard-called genotype files. Only bi-allelic SNPs with MAF > 0.01, HWE $P > 0.01$, and INFO > 0.80 were included. Independent LD-based groups of SNPs were identified using European populations linkage disequilibrium patterns from 1000 G (genome build GRCh37) and the NIH National Cancer Institute SNP clip Tool (https://ldlink.nci.nih.gov/?tab=snpclip).

Phenotype data. Descriptive information on cases and controls can be found in Supplementary Table 4.

Information on individual survival status up to May 1st, 2022, was retrieved from the Danish Central Population Register[73].

Self-reported age at menopause was collected as part of comprehensive interviews in the 1905, 1910, and 1915 birth cohort studies and MADT, focusing on health and lifestyle issues and assessments of cognitive and physical abilities. Among the younger controls, age at menopause was available for 529 women (mean = 49.5 years, sd = 5.1 years, and range = 35–65 years), and among the long-lived individuals for 282 women (mean = 49.4 year, sd = 4.6 years, and range = 35–60 years). Women with self-reported age at menopause <35 years ($N = 15$) or >65 years ($N = 1$, 71 years) were excluded. In general, applying these exclusion criteria resulted in an attenuation of effect sizes, primarily for positively associated SNPs.

Analyses. The association between longevity and SNP minor allele dosage (coded as 0, 1, or 2 depending on the number of minor alleles) was analyzed in STATA v. 17.0 using a logistic regression model including sex as a covariate and with twin pair number as a random effect to account for the relatedness between twins from the same twin pair. *OSER1* SNPs associated ($P < 0.05$) with longevity. The analysis was performed using a logistic regression model comparing long-lived

cases to younger controls and including sex as a covariate. *P*-values are uncorrected.

The association between age at menopause and SNP minor allele dosage (coded as 0, 1, or 2 depending on the number of minor alleles) was analyzed in STATA v. 17.0 using a linear regression model with twin pair number as a random effect to account for the relatedness between twins from the same twin pair in the analysis of the younger controls. OSER1 SNPs associated ($P < 0.05$) with age at menopause. The analysis was performed in long-lived and younger women using a linear regression model. *P*-values are uncorrected.

A Bonferroni-corrected significance level of $P < 0.0024$ (corresponding to correction for 21 tests; seven independent LD-based groups of SNPs, two phenotypes, one study cohort for longevity, and two study cohorts for age at menopause) was applied. However, given the a priori hypothesis of an association between *OSER1* and longevity and fertility/age at menopause, uncorrected *P*-values are reported.

Statistics & reproducibility

Scatter plots were analyzed using Prism 9 and presented as mean ± SD. Survival curves were generated and analyzed by Log-rank (Mantel-Cox) test using Prism 9. Significant differences between treatments/groups were analyzed using a Student's *t*-test, one-way ANOVA, or two-way ANOVA: $*p < 0.05$; $**p < 0.01$; $***p < 0.001$; $****p < 0.0001$. No data were excluded from the analyses. The experiments were randomized. The investigators were not blinded to allocation during experiments and outcome assessment except for the immunofluorescence analysis.

Reporting summary

Further information on research design is available in the Nature Portfolio Reporting Summary linked to this article.

Data availability

The numerical data and uncropped representative images used for quantifications are available as Source Data file accompanying this paper. Other data reported in the current study can be found in the Supplementary Information. All cellular and animal data are available from the corresponding author upon reasonable request. The transcriptomics raw sequence reads data for *BmFoxO* knockdown and overexpression can be found at PRJNA943622. RNA-Seq data for Control (Accession No. SRX20534814), BmFoxO-RNAi (Accession No. SRX20534813), and FoxOCA-OE (Accession No. SRX20534812). The transcriptomics raw data for *BmOSER1* overexpression silkworms (NCBI BioProject Accession #: PRJNA978397) and *Ceoser1* knockdown *C. elegans* (NCBI BioProject Accession #: PRJNA978499) are available at NCBI. The mass spectrometry proteomics data have been deposited to the ProteomeXchange Consortium via the PRIDE partner repository with the dataset identifier PXD036579. According to the Danish and EU legislations, transfer and sharing of individual-level data require prior approval from the Research & Innovation Organization at the University of Southern Denmark or the Danish Data Protection Agency and require that data sharing requests be dealt with on a case-by-case basis. For this reason, the raw data cannot be deposited in a public database. However, we welcome any inquiries regarding collaboration and individual requests for data sharing. Inquiries and requests can be sent to Marianne Nygaard (mnygaard@health.sdu.dk). Further information about data access can be found here: https://www.sdu.dk/en/om-sdu/institutter-centre/ist_sundhedstjenesteforsk/centre/dtr/researcher. Source data are provided with this paper.

References

1. van der Horst, A. & Burgering, B. M. Stressing the role of FoxO proteins in lifespan and disease. *Nat. Rev. Mol. Cell Biol.* **8**, 440–450 (2007).
2. Martins, R., Lithgow, G. J. & Link, W. Long live FOXO: unraveling the role of FOXO proteins in aging and longevity. *Aging Cell* **15**, 196–207 (2016).
3. Kenyon, C. J. The genetics of ageing. *Nature* **464**, 504–512 (2010).
4. Greer, E. L. et al. The energy sensor AMP-activated protein kinase directly regulates the mammalian FOXO3 transcription factor. *J. Biol. Chem.* **282**, 30107–30119 (2007).
5. Hay, N. Interplay between FOXO, TOR, and Akt. *Bba-Mol. Cell Res* **1813**, 1965–1970 (2011).
6. Robida-Stubbs, S. et al. TOR Signaling and Rapamycin Influence Longevity by Regulating SKN-1/Nrf and DAF-16/FoxO. *Cell Metab.* **15**, 713–724 (2012).
7. Jiang, Y., Yan, F., Feng, Z., Lazarovici, P. & Zheng, W. Signaling Network of Forkhead Family of Transcription Factors (FOXO) in Dietary Restriction. *Cells-Basel* **9**. https://doi.org/10.3390/cells9010100 (2019)
8. Mukhopadhyay, A., Oh, S. W. & Tissenbaum, H. A. Worming pathways to and from DAF-16/FOXO. *Exp. Gerontol.* **41**, 928–934 (2006).
9. Dansen, T. B. & Burgering, B. M. T. Unravelling the tumor-suppressive functions of FOXO proteins. *Trends Cell Biol.* **18**, 421–429 (2008).
10. Manolopoulos, K. N., Klotz, L. O., Korsten, P., Bornstein, S. R. & Barthel, A. Linking Alzheimer's disease to insulin resistance: the FoxO response to oxidative stress. *Mol. Psychiatr.* **15**, 1046–1052 (2010).
11. Hwang, I. et al. FOXO protects against age-progressive axonal degeneration. *Aging Cell* **17**. https://doi.org/10.1111/acel.12701 (2018)
12. Du, S. & Zheng, H. Role of FoxO transcription factors in aging and age-related metabolic and neurodegenerative diseases. *Cell Biosci.* **11**, 188 (2021).
13. Sosa, V. et al. Oxidative stress and cancer: an overview. *Ageing Res Rev.* **12**, 376–390 (2013).
14. Daenen, K. et al. Oxidative stress in chronic kidney disease. *Pediatr. Nephrol.* **34**, 975–991 (2019).
15. Niedzielska, E. et al. Oxidative Stress in Neurodegenerative Diseases. *Mol. Neurobiol.* **53**, 4094–4125 (2016).
16. Klotz, L. O. et al. Redox regulation of FoxO transcription factors. *Redox Biol.* **6**, 51–72 (2015).
17. Nemoto, S. & Finkel, T. Redox regulation of forkhead proteins through a p66shc-dependent signaling pathway. *Science* **295**, 2450–2452 (2002).
18. Kops, G. J. et al. Forkhead transcription factor FOXO3a protects quiescent cells from oxidative stress. *Nature* **419**, 316–321 (2002).
19. Chen, C. C. et al. FoxOs inhibit mTORC1 and activate Akt by inducing the expression of Sestrin3 and Rictor. *Dev. Cell* **18**, 592–604 (2010).
20. Lee, J. H. et al. Sestrin as a Feedback Inhibitor of TOR That Prevents Age-Related Pathologies. *Science* **327**, 1223–1228 (2010).
21. Hagenbuchner, J. et al. FOXO3-induced reactive oxygen species are regulated by BCL2L11 (Bim) and SESN3. *J. Cell Sci.* **125**, 1191–1203 (2012).
22. Ferber, E. C. et al. FOXO3a regulates reactive oxygen metabolism by inhibiting mitochondrial gene expression. *Cell Death Differ.* **19**, 968–979 (2012).
23. Li, Z., Anugula, S. & Rasmussen, L. J. in *Aging* 275-295 (Elsevier, 2023).
24. Lee, S. S., Kennedy, S., Tolonen, A. C. & Ruvkun, G. DAF-16 target genes that control C. elegans life-span and metabolism. *Science* **300**, 644–647 (2003).
25. Alic, N. et al. Genome-wide dFOXO targets and topology of the transcriptomic response to stress and insulin signalling. *Mol. Syst. Biol.* **7**, 502 (2011).

26. Audesse, A. J. et al. FOXO3 directly regulates an autophagy network to functionally regulate proteostasis in adult neural stem cells. *Plos Genet.* **15**, e1008097 (2019).
27. Eijkelenboom, A. et al. Genome-wide analysis of FOXO3 mediated transcription regulation through RNA polymerase II profiling. *Mol. Syst. Biol.* **9**, 638 (2013).
28. Webb, A. E., Kundaje, A. & Brunet, A. Characterization of the direct targets of FOXO transcription factors throughout evolution. *Aging Cell* **15**, 673–685 (2016).
29. Song, J. et al. Genome-wide identification and characterization of Fox genes in the silkworm, Bombyx mori. *Funct. Integr. Genomics* **15**, 511–522 (2015).
30. Li, Y. et al. Transcriptome analysis of the silkworm (Bombyx mori) by high-throughput RNA sequencing. *Plos One* **7**, e43713 (2012).
31. Duttaroy, A. et al. The manganese superoxide dismutase gene of Drosophila: structure, expression, and evidence for regulation by MAP kinase. *DNA Cell Biol.* **16**, 391–399 (1997).
32. Paul, A. & Duttaroy, A. Genomic regions responsible for manganese superoxide dismutase regulation in Drosophila melanogaster. *Aging Cell* **2**, 223–231 (2003).
33. Tang, H. & Pang, S. Proline Catabolism Modulates Innate Immunity in Caenorhabditis elegans. *Cell Rep.* **17**, 2837–2844 (2016).
34. Kenyon, C., Chang, J., Gensch, E., Rudner, A. & Tabtiang, R. A C. elegans mutant that lives twice as long as wild type. *Nature* **366**, 461–464 (1993).
35. Friedman, D. B. & Johnson, T. E. A mutation in the age-1 gene in Caenorhabditis elegans lengthens life and reduces hermaphrodite fertility. *Genetics* **118**, 75–86 (1988).
36. Uno, M. et al. Neuronal DAF-16-to-intestinal DAF-16 communication underlies organismal lifespan extension in C. elegans. *iScience* **24**, 102706 (2021).
37. Lakowski, B. & Hekimi, S. The genetics of caloric restriction in Caenorhabditis elegans. *Proc. Natl. Acad. Sci. USA* **95**, 13091–13096 (1998).
38. Itoh, K., Ye, P., Matsumiya, T., Tanji, K. & Ozaki, T. Emerging functional cross-talk between the Keap1-Nrf2 system and mitochondria. *J. Clin. Biochem Nutr.* **56**, 91–97 (2015).
39. Tan, B. L., Norhaizan, M. E., Liew, W. P. & Sulaiman Rahman, H. Antioxidant and Oxidative Stress: A Mutual Interplay in Age-Related Diseases. *Front Pharm.* **9**, 1162 (2018).
40. Calnan, D. R. & Brunet, A. The FoxO code. *Oncogene* **27**, 2276–2288 (2008).
41. Shama, S., Lai, C. Y., Antoniazzi, J. M., Jiang, J. C. & Jazwinski, S. M. Heat stress-induced life span extension in yeast. *Exp. Cell Res.* **245**, 379–388 (1998).
42. Lithgow, G. J., White, T. M., Melov, S. & Johnson, T. E. Thermotolerance and Extended Life-Span Conferred by Single-Gene Mutations and Induced by Thermal-Stress. *P Natl. Acad. Sci. USA* **92**, 7540–7544 (1995).
43. Morley, J. F. & Morimoto, R. I. Regulation of longevity in Caenorhabditis elegans by heat shock factor and molecular chaperones. *Mol. Biol. Cell* **15**, 657–664 (2004).
44. Hsu, A. L., Murphy, C. T. & Kenyon, C. Regulation of aging and age-related disease by DAF-16 and heat-shock factor. *Science* **300**, 1142–1145 (2003).
45. Lee, S. J., Murphy, C. T. & Kenyon, C. Glucose Shortens the Life Span of C. elegans by Downregulating DAF-16/FOXO Activity and Aquaporin Gene Expression. *Cell Metab.* **10**, 379–391 (2009).
46. Mustafi, S. B., Chakraborty, P. K., Dey, R. S. & Raha, S. Heat stress upregulates chaperone heat shock protein 70 and antioxidant manganese superoxide dismutase through reactive oxygen species (ROS), p38MAPK, and Akt. *Cell Stress Chaperon-.* **14**, 579–589 (2009).
47. Zhang, Q., Kopp, M., Babiak, I. & Fernandes, J. M. O. Low incubation temperature during early development negatively affects survival and related innate immune processes in zebrafish larvae exposed to lipopolysaccharide. *Sci. Rep.* **8**, 4142 (2018).
48. Pan, M. H. et al. Establishment and characterization of an ovarian cell line of the silkworm, Bombyx mori. *Tissue Cell* **42**, 42–46 (2010).
49. Lynn, D. E. Methods for maintaining insect cell cultures. *J. Insect Sci.* **2**, 9 (2002).
50. Rhiel, M., MitchellLogean, C. M. & Murhammer, D. W. Comparison of Trichoplusia ni BTI-Tn-5B1-4 (High Five((TM))) and Spodoptera frugiperda Sf-9 insect cell line metabolism in suspension cultures. *Biotechnol. Bioeng.* **55**, 909–920 (1997).
51. Edgar, R. C. MUSCLE: multiple sequence alignment with high accuracy and high throughput. *Nucleic Acids Res.* **32**, 1792–1797 (2004).
52. Ronquist, F. & Huelsenbeck, J. P. MrBayes 3: Bayesian phylogenetic inference under mixed models. *Bioinformatics* **19**, 1572–1574 (2003).
53. Ronquist, F. et al. MrBayes 3.2: efficient Bayesian phylogenetic inference and model choice across a large model space. *Syst. Biol.* **61**, 539–542 (2012).
54. Sun, W. et al. Phylogeny and evolutionary history of the silkworm. *Sci. China Life Sci.* **55**, 483–496 (2012).
55. Nylander, J. A., Wilgenbusch, J. C., Warren, D. L. & Swofford, D. L. AWTY (are we there yet?): a system for graphical exploration of MCMC convergence in Bayesian phylogenetics. *Bioinformatics* **24**, 581–583 (2008).
56. Song, J. et al. Astragalus Polysaccharide Extends Lifespan via Mitigating Endoplasmic Reticulum Stress in the Silkworm, Bombyx mori. *Aging Dis.* **10**, 1187–1198 (2019).
57. Wang, G. H. et al. Reference genes identified in the silkworm Bombyx mori during metamorphism based on oligonucleotide microarray and confirmed by qRT-PCR. *Insect Sci.* **15**, 405–413 (2008).
58. Bustin, S. A. et al. The MIQE guidelines: minimum information for publication of quantitative real-time PCR experiments. *Clin. Chem.* **55**, 611–622 (2009).
59. Eichenlaub, T. et al. Warburg Effect Metabolism Drives Neoplasia in a Drosophila Genetic Model of Epithelial Cancer. *Curr. Biol.* **28**, 3220–3228.e3226 (2018).
60. Gut, P. & Verdin, E. The nexus of chromatin regulation and intermediary metabolism. *Nature* **502**, 489–498 (2013).
61. Pietrocola, F., Galluzzi, L., Bravo-San Pedro, J. M., Madeo, F. & Kroemer, G. Acetyl coenzyme A: a central metabolite and second messenger. *Cell Metab.* **21**, 805–821 (2015).
62. Zhou, L., He, B., Deng, J., Pang, S. & Tang, H. Histone acetylation promotes long-lasting defense responses and longevity following early life heat stress. *Plos Genet* **15**, e1008122 (2019).
63. Brenner, S. The genetics of Caenorhabditis elegans. *Genetics* **77**, 71–94 (1974).
64. Pang, S. & Curran, S. P. Adaptive capacity to bacterial diet modulates aging in C. elegans. *Cell Metab.* **19**, 221–231 (2014).
65. Moparthi, L. & Koch, S. A uniform expression library for the exploration of FOX transcription factor biology. *Differentiation* **115**, 30–36 (2020).
66. Bekker-Jensen, D. B. et al. A Compact Quadrupole-Orbitrap Mass Spectrometer with FAIMS Interface Improves Proteome Coverage in Short LC Gradients. *Mol. Cell Proteom.* **19**, 716–729 (2020).
67. Rasmussen, S. H. et al. Cohort Profile: The 1895, 1905, 1910 and 1915 Danish Birth Cohort Studies - secular trends in the health and functioning of the very old. *Int J. Epidemiol.* **46**, 1746 (2017).

68. Robine, J. M. et al. Centenarians Today: New Insights on Selection from the 5-COOP Study. *Curr. Gerontol. Geriatr. Res* **2010**, 120354 (2010).
69. Pedersen, D. A. et al. The Danish Twin Registry: An Updated Overview. *Twin Res Hum. Genet* **22**, 499–507 (2019).
70. Miller, S. A., Dykes, D. D. & Polesky, H. F. A simple salting out procedure for extracting DNA from human nucleated cells. *Nucleic acids Res.* **16**, 1215 (1988).
71. Howie, B. N., Donnelly, P. & Marchini, J. A flexible and accurate genotype imputation method for the next generation of genome-wide association studies. *Plos Genet* **5**, e1000529 (2009).
72. Chang, C. C. et al. Second-generation PLINK: rising to the challenge of larger and richer datasets. *Gigascience* **4**, 7 (2015).
73. Pedersen, C. B., Gotzsche, H., Moller, J. O. & Mortensen, P. B. The Danish Civil Registration System. A cohort of eight million persons. *Dan. Med Bull.* **53**, 441–449 (2006).

Acknowledgements

We thank Dr. Shilin Song and Prof. Shanshan Pang (Chongqing University), Kaige Hao, Tao Sun, Li Xiao, and Yunzhu Shang for their generous technical support with *D. melanogaster*, *C. elegans*, and *B. mori* assays. We would also like to thank associate Professor Stefan Koch from the Department of Biomedical and Clinical Sciences (BKV), Linköping University, Sweden, for generously sharing pCS2, FOXO1, FOXO3, FOXO4, FOXO6 plasmids. We also thank BioMedVisual.com for helping with the working model illustrations. We express our sincere gratitude to the editors and anonymous reviewers for their meticulous examination and valuable feedback on our manuscript. This work is supported by grants from the National Natural Science Foundation of China (Grant Nos. 32272939, 32330102, and 31902215), Natural Science Foundation of Chongqing, China (Grant no. cstc2021jcyj-cxttX0005), and Funds of China Agriculture Research System of MOF and MARA (No. CARS-18-ZJ0102). L.J.R. receives financial support from the Nordea-Fonden and Novo Nordisk Foundation (NNF23OC0084974 and NNF17OC0027812). L.J.R. is a member of the Clinical Academic Group: Recovery Capacity After Acute Illness in An Aging Population (RECAP). The studies behind the individuals included here received funding from The National Program for Research Infrastructure 2007 (grant no. 09-063256) from the Danish Agency for Science Technology and Innovation, the Velux Foundation, the US National Institute of Health (P01 AG08761), the Danish Agency for Science, Technology and Innovation/The Danish Council for Independent Research (grant no. 11-107308), the European Union's Seventh Framework Programme (FP7/2007-2011) under grant agreement n° 259679, the INTERREG 4 A programme Syddanmark-Schleswig-K.E.R.N. (by EU funds from the European Regional Development Fund), the CERA Foundation (Lyon), and the AXA Research Fund, Paris. Genotyping of data set 2 was conducted by the SNP&SEQ Technology Platform, Science for Life Laboratory, Uppsala, Sweden (http://snpseq.medsci.uu.se/genotyping/snp-services/) and supported by NIH R01 AG037985. L.Z. is supported by a grant from NSFC (No. 32000810). V.A.B. receives financial support from the Nordea-fonden and Novo Nordisk Foundation (NNF17OC0027812). Z.Y. was supported by the Nonprofit Central Research Institute Fund of the Chinese Academy of Medical Sciences (grant no. 2023-RC180-03), the Chinese Academy of Medical Sciences (CAMS) Innovation Fund for Medical Sciences (2022-I2M-2-004, 2023-I2M-2-005) and the NCTIB Fund for the R&D Platform for Cell and Gene Therapy. Work at The Novo Nordisk Foundation Center for Protein Research (CPR) was funded in part by a donation from the Novo Nordisk Foundation (NNF14CC0001).

Author contributions

J.S.: Conceptualization, Methodology, Validation, Formal analysis, Investigation, Data Curation, Writing - Original Draft, Writing - Review & Editing, Visualization, Project administration, Funding acquisition. Z.L.: Conceptualization, Methodology, Validation, Formal analysis, Investigation, Data Curation, Writing - Original Draft, Writing - Review & Editing, Visualization, Project administration, Funding acquisition. L.Z.: Methodology, Validation, Formal analysis, Investigation, Data Curation, Writing - Review & Editing, Funding acquisition. X.C.: Methodology, Validation, Formal analysis, Investigation, Data Curation, Writing - Review & Editing. W.Q.G.S.: Methodology, Validation, Formal analysis, Investigation, Data Curation, Writing - Review & Editing. H.H.: Methodology, Resources, Writing - Review & Editing, Funding acquisition. Z.Y.: Methodology, Validation, Formal analysis, Investigation, Data Curation, Writing - Review & Editing, Visualization. J.V.O.: Resources, Writing - Review & Editing, Funding acquisition. Y.L.: Methodology, Validation, Formal analysis, Investigation, Data Curation, Writing - Review & Editing. M.N.: Methodology, Validation, Formal analysis, Investigation, Data Curation, Writing - Review & Editing, Funding acquisition. K.C.: Methodology, Validation, Formal analysis, Investigation, Data Curation, Writing - Review & Editing, Funding acquisition. X.T.: Writing - Review & Editing. V.A.B.: Writing - Review & Editing, Funding acquisition. L.J.R.: Conceptualization, Resources, Writing - Original Draft, Writing - Review & Editing, Supervision, Project administration, Funding acquisition. F.D.: Conceptualization, Resources, Writing - Original Draft, Writing - Review & Editing, Supervision, Project administration, Funding acquisition.

Competing interests

The authors declare no competing interests.

Additional information

Supplementary information The online version contains supplementary material available at https://doi.org/10.1038/s41467-024-51542-z.

Correspondence and requests for materials should be addressed to Lene Juel Rasmussen or Fangyin Dai.

Peer review information *Nature Communications* thanks the anonymous reviewers for their contribution to the peer review of this work.

[1]State Key Laboratory of Resource Insects, Key Laboratory for Sericulture Biology and Genetic Breeding, Ministry of Agriculture and Rural Affairs, College of Sericulture, Textile and Biomass Sciences, Southwest University, Chongqing 400715, China. [2]Center for Healthy Aging, Department of Cellular and Molecular Medicine, University of Copenhagen, 2200 Copenhagen, Denmark. [3]Department of Cellular and Molecular Medicine, University of Copenhagen, 2200 Copenhagen, Denmark. [4]Novo Nordisk Foundation Center for Protein Research, University of Copenhagen, 2200 Copenhagen, Denmark. [5]Key Laboratory of Common Mechanism Research for Major Diseases, Suzhou Institute of Systems Medicine, Chinese Academy of Medical Sciences & Peking Union Medical College, Suzhou, China. [6]Epidemiology, Biostatistics and Biodemography, Department of Public Health, University of Southern Denmark, Odense, Denmark. [7]Department of Clinical Genetics, Odense University Hospital, Odense, Denmark. [8]Department of Clinical Biochemistry, Odense University Hospital, Odense, Denmark. [9]Section on DNA repair, National Institute on Aging, National Institutes of Health, Baltimore, MD 21224, USA. [10]These authors contributed equally: Jiangbo Song, Zhiquan Li. ✉e-mail: lenera@sund.ku.dk; fydai@swu.edu.cn